Functionalization of cellulosic fibers with a kaolinite-TiO2 nano-hybrid composite via a solvothermal process for flame retardant applications

Carlos Rafael Silva de Oliveira, Marcos Batistella, Selene Maria de Arruda Guelli Ulson de Souza, Antônio Augusto Ulson de Souza

Functionalization of cellulosic fibers with a kaolinite-TiO_2 nano-hybrid composite *via* a solvothermal process for flame retardant applications

Carlos Rafael Silva de Oliveira [a,*], Marcos Antonio Batistella [a,b], Selene Maria de Arruda Guelli Ulson de Souza [a], Antônio Augusto Ulson de Souza [a]

[a] *Federal University of Santa Catarina, Chemical Engineering Department, Mass Transfer Laboratory, PO Box 476, 88.040-900 Florianópolis, SC, Brazil*
[b] *IMT Mines Alès, PCH-Polymer Composites Hybrids, 6 Avenue de Clavières, 30319 Alès Cedex, France*

A B S T R A C T

Eco-responsible flame retardant treatments with some resistance to washing are of considerable interest in the sale and applications of technical garments and home textiles. Thus, in the present study, a nano-hybrid composite based on kaolinite-TiO_2 was prepared and incorporated into the fibers of cotton fabric through a more sustainable route compared to existing commercial processes. SEM analyses revealed a mineral covering of the treated cotton fibers, which do not propagate flames when exposed to fire and have a self-extinguishing behavior after the heat source removal. The method proved to be efficient in obtaining a cotton product with high fireproof performance. It was observed that after functionalization, the fabric showed a thermal degradation 41% less at 800 °C, an increase in the residue formation, and a reduction of about 85% in peak heat release measured by PCFC. Some resistance to washing was noticed, and the mechanical resistance of fibers was preserved.

Keywords:
Flame retardants
Cotton fabric
Mineral composite
Kaolinite
Titanium dioxide

Chemical compounds studied in this article:
Kaolinite (PubChem CID: 71300855)
Titanium dioxide (PubChem CID: 26042)
3-Aminopropyltriethoxysilane (PubChem CID: 13521)
Sulfuric Acid (PubChem CID: 1118)
Glacial Acetic Acid (PubChem CID: 176)
Phosphoric Acid (PubChem CID: 1004)
Ethanol (PubChem CID: 702)
Urea (PubChem CID: 1176)
Sodium Hydroxide (PubChem CID: 14798)

1. Introduction

Cotton fiber is the most important natural fiber. Its cultivation and consumption correspond to more than 82% of the total cultivation and natural fibers consumption on the planet (Baydar et al., 2015; Günther et al., 2017). Cotton represents about 33% of fiber volume (natural, artificial, and synthetic) produced worldwide consumed for textile purposes (Baydar et al., 2015; FAO ICAC, 2013; Günther et al., 2017). Chemically, the cotton fiber consists, basically, of cellulose, a highly combustible and easily flammable polysaccharide (Jabli et al., 2018; Klemm et al., 2005; Sebeia et al., 2021; Tka et al., 2018). However, textiles can be considered as one of the most flammable materials found in fire situations. Considering that 70% to 90% of fire deaths occur in domestic environments (in which the presence and use of textiles are very common) the homes are the places with the highest risk of fire accidents (Olawoyin, 2018; Thompson et al., 2018; Zhao et al., 2017). The flammability of fabrics is governed by their composition, which, in most cases, is made of highly flammable polymers such as cotton (Bajaj, 1992; Menachem & Pearce, 2006; Zhu et al., 2004). For these reasons, there has been a growing concern in search for fireproof solutions that can be applied to these materials sustainably and economically, through finishes that present effective performance and some durability (Horrocks et al., 2005; Huang et al., 2015; Zhao et al., 2017).

Currently, the treatments considered as durable, *i.e.*, those that resist domestic washing, use mostly toxic chemical agents or polluting application routes (*e.g.*, based on formaldehyde and antimony oxide III), some are bioaccumulative as in the case of halogenates, dangerous to health and the environment (Ali et al., 2011; Skinner, 2011; Takigami et al., 2009). For these reasons, the search for effective and more sustainable treatments applied to cellulosic materials to replace the current ones has

* Corresponding author.
E-mail addresses: carlos.oliveira@posgrad.ufsc.br (C.R.S. de Oliveira), marcos.batistella@mines-ales.fr (M.A. Batistella), selene.souza@ufsc.br (S.M.A. Guelli Ulson de Souza), antonio.augusto.souza@ufsc.br (A.A. Ulson de Souza).

been the motivator of research over the last twenty years (Al-Mosawi et al., 2015; *Handbook of Fire Resistant Textiles,* 2013; Horrocks et al., 2005). In addition to the study of phosphorus and nitrogen compounds applied to cellulose, recent research has explored other natural additives, such as silicon compounds and metal oxides that have shown great potential for semi-durable flame retardant applications (Horrocks et al., 2005; Montazer & Harifi, 2018; Verbič et al., 2019). Efforts in this regard have proven the synergistic action of the blends of these components during combustion, which can retarding and/or extinguishing the spread of flames in polymeric materials (Mngomezulu et al., 2014; Uddin et al., 2015; Wang et al., 2017). However, few works have been done with the application in natural fibers, such as cotton.

Some research with aluminosilicates and metal oxides has revealed that the mode of action occurs by physical effect, *i.e.*, it depends directly on the particle chemical nature, the matrix, particle size, porosity, concentration of OH groups on the surface, surface area, and crystal density (De Oliveira et al., 2021; Mngomezulu et al., 2014). During combustion, these additives can accelerate the formation of a superficial carbonaceous layer, preventing or hindering the heat and mass transfer (free radicals released by the fiber pyrolysis) between the substrate and the gas phase (Kiliaris & Papaspyrides, 2010; Mngomezulu et al., 2014; Ribeiro et al., 2018). Clay minerals can also have an intumescent action with the formation of an expanded carbon-mineral layer capable of shielding the polymer matrix, hindering gas exchange/heat between the combustion stages and resulting in the flame extinguishing (De Oliveira et al., 2021).

Metal oxides nanoparticles (Saleh, 2020), for example, iron oxide (Fe_2O_3), aluminum oxide (Al_2O_3), zinc oxide (ZnO), and titanium dioxide (TiO_2), may have flame retardant action depending on their applied concentration, particle size, and surface area (Gallo et al., 2009, 2011; Laachachi et al., 2005, 2007; Lewin, 2001; Mngomezulu et al., 2014). Among these metal oxides, titania has some advantages, as it can decrease the transfer of oxygen to the condensed phase, reducing the oxidative attack of the polymer chain (Peng et al., 2017). However, recent works show that these materials, when applied alone, may not satisfactorily combat combustion but act synergistically increasing the performance when mixed with other FRs compounds, such as phosphorus and nitrogen, resulting in a formulation of intumescent action (Gallo et al., 2011; Laachachi et al., 2007; Mngomezulu et al., 2014). Moreover, some studies with titania have shown that it also has a high capacity to absorb UV radiation. This property acts as a shield that protects the polymer and other FRs (Flame Retardants) additives from UV and consequent aging, extending the useful life of finishing and material.

Titania has received attention in the literature, and some works evaluated getting composites based on kaolinite and titania with photocatalytic applications of drugs and dyes degradation, dyes and heavy metals adsorbents from wastewater, antimicrobial action, and others (Hai et al., 2015; Kibanova et al., 2009; Li et al., 2018; Mamulová Kutlákova et al., 2011; Tokarský et al., 2012; Wang et al., 2011). However, to the best of our knowledge, no one deals with the use of kaolinite-TiO_2 composite incorporated into cotton for flame retardation purposes. Therefore, the objective of the present study was to test the use of a nano-hybrid composite based on kaolinite-TiO_2 (developed by the authors in previous work (de Oliveira et al., 2020)) as a flame-retardant additive incorporated into the cotton fabric, and the maintenance of this property after washing cycles.

2. Experimental section

2.1. Materials

Serge 2 × 1 pre-bleached plain-woven fabric (100% cotton), kindly supplied by PARANATEX Têxtil Brazilian company (20 picks·cm^{-1} in weft; 35 ends·cm^{-1} in warp; fabric grammage 314 g·m^{-2}), was used as substrate. After mercerization, the fabric samples were cut into 30 cm × 7.6 cm (according to ASTM D6413-08). Kaolinite under the trade name Saca-B® was provided by IMERYS do Brasil Comércio de Extração de Minérios Ltda. Titanium dioxide under the name AEROXIDE® TiO_2 P25 was obtained by Evonik do Brasil Ltda. (3-aminopropyl) triethoxysilane (APTES) 99% was purchased by Sigma-Aldrich (Merck). An emulgator PROTE-PON WR140 – BR© was supplied by PROX do Brasil Ltda. AATCC 1993 Standard Reference Soap was received from donation by Federal Institute of Santa Catarina (Campus Araranguá - Brazil). Sulfuric Acid 98% and Glacial Acetic Acid 100% were purchased by LabSynth Ltda (Brazil). Phosphoric Acid 85% was supplied by Vetec Ltda (Brazil). Absolute Ethyl Alcohol 99.8% and pure Urea were purchased by Neon Ltda (Brazil). Sodium Hydroxide (pearly solid) was provided by Lafan Ltda (Brazil).

2.2. Experimental procedure

The proposed methodology occurs in two steps. The first step consists of the fabric preparation by mercerization and the preparation of a nanostructured composite based on kaolinite and titania (see de Oliveira et al. (2020)). The second step consists of incorporating the composite into the cotton fabric. The kaolinite-TiO_2 composite called "KT" is functionalized with APTES by a solvothermal reaction followed by the incorporation of the functionalized particles into the fabric samples. This sample is named T2 through the text. For comparison, pure kaolinite called "PK" is incorporated on fabric by the same method used for KT (in the second step). This sample is named T1.

2.2.1. Mercerization of pre-bleached raw cotton fabric – 1st step

The pre-bleached raw cotton fabric called "BRF" was submitted to a mercerization process in a laboratory Jigger WJ-B-350 (Mathis). The mercerization process was carried out at 30 °C for 2 h using a bath ratio of 1:6 (kg of fabric:L of bath). For mercerization, a solution of 10% sodium hydroxide with PROTE-PON WR140 - BR© (1 g·L^{-1}) emulsifier in distilled water was prepared. After mercerization, the fabric was neutralized with a glacial acetic acid solution (2% v/v), at 30 °C for 30 min. Subsequently, the fabric was rinsed three times with tap water at 30 °C for 10 min. Finally, the fabric was removed from the equipment and subjected to hydro extraction in a laboratory Padder-Foulard FVH (Mathis). The hydro extraction process was carried out at room temperature, with a squeezing pressure of 2 bar and a speed of 1 m·min^{-1}. Then, the mercerized raw fabric (MRF) obtained was dried in a laboratory Stenter LTE-S (Mathis) at 85 °C for 5 min.

2.2.2. Obtaining the KT composite – 1st step

The procedure for obtaining the composite is described (in detail) in a previous work (de Oliveira et al., 2020). Basically, distilled water (61 mL) was poured into a 250 mL beaker. TiO_2 (15 g) was slowly added to the water and the beaker was kept under stirring for 30 min. After that, the beaker was kept in a container with ice under vigorous magnetic stirring. Sulfuric acid (30 mL) was slowly added to the mixture for 30 min, and the mixture was kept under constant stirring at 80 °C for 1 h and 30 min. A white gelatinous dispersion (sol-gel) of sulfated TiO_2 was obtained and the product was reserved in amber glass and kept at room temperature.

Briefly, the reaction to obtain the composite was carried out in a jacketed glass reactor. For this, distilled water (200 mL) and PK (20 g, i.e., 10% w/v) were added to the reactor and kept under constant stirring. At 90 °C, sulfated TiO_2 sol-gel (50 mL, *i.e.*, 25% v/v) was slowly dripped and maintained at 90 °C for 24 h. After reaction time, the solid material was thoroughly washed with distilled water and the supernatant was discarded. The KT composite was washed until the wash water had a conductivity lower than $1 \cdot 10^2$ μS·cm^{-1}, to ensure that all sulfate ions were removed. Finally, the KT composite was dried at 50 °C for 3 h using a laboratory oven; then the solid was easily milled with a porcelain pistil, and reserved in a glass container. An illustration of the system for obtaining the KT composite is shown in Fig. 1A.

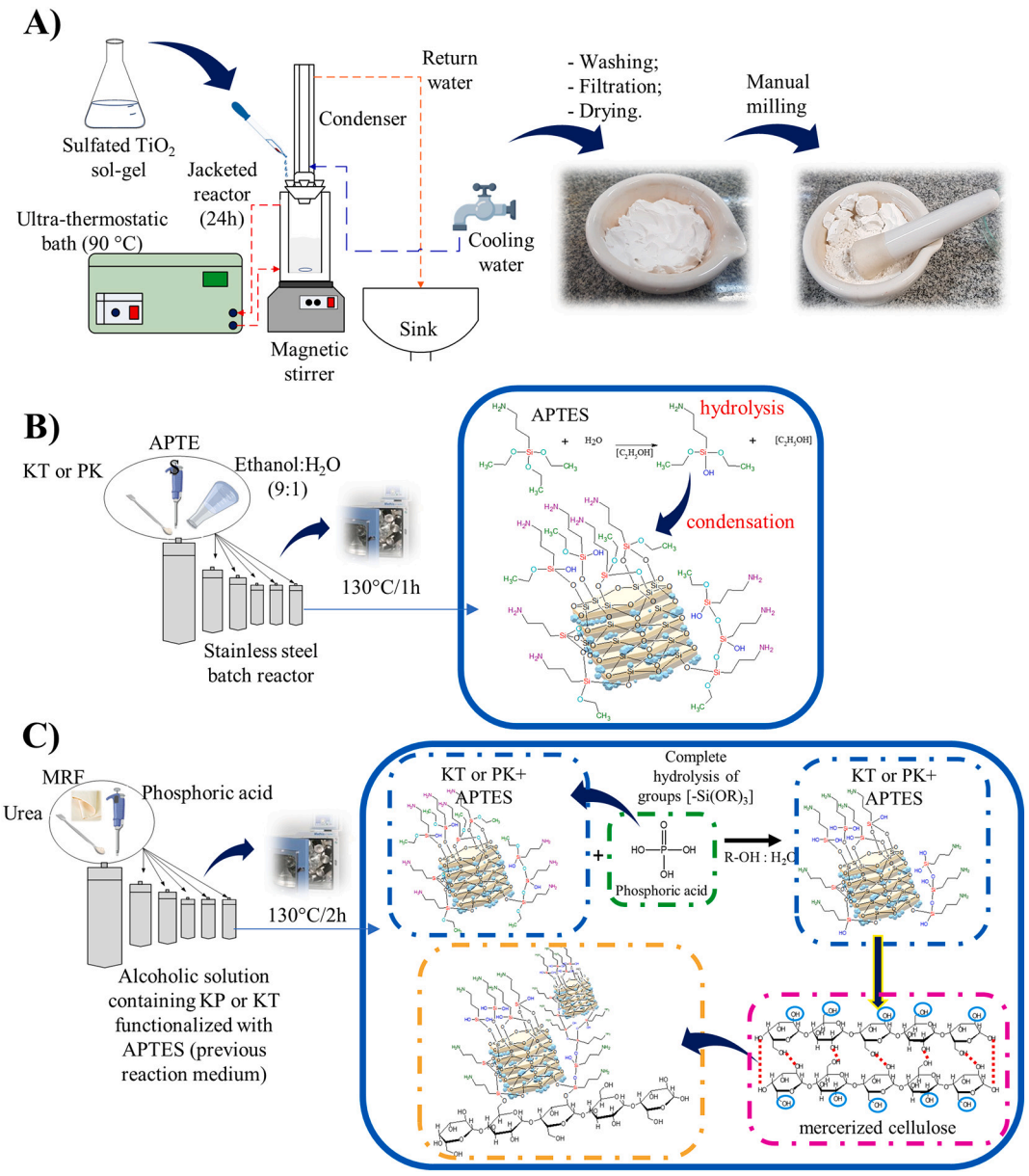

Fig. 1. (A) - Schematic illustration of the experimental procedure for preparing the KT composite; (B) - Schematic illustration of the experimental procedure for preparing the silanized KT and PK particles (the reactions that occur in this step are illustrated on the right); and (C) - Schematic illustration of the experimental procedure for preparing of T1 and T2 samples (the reactions that occur in this step are illustrated on the right).

2.2.3. Obtaining the flame retardant finishing of cotton fabric – 2nd step

At first, silanization of the KT particles was carried out in an ethanol-H_2O medium. Briefly, ethyl alcohol (90 mL) and distilled water (10 mL) were measured and spilled into a stainless-steel reactor where the batch reaction occurred. In the medium the particles (1.0 g, *i.e.*, 1.0% w/v) and APTES (800 µL, *i.e.*, 0.8% v/v) were added (the same method was used for the silanization of PK particles). The reactor was closed and inserted in an HT ALT-I (Mathis) equipment where it remained at 130 °C for 1 h under constant agitation with a rotation speed of 40 RPM (Fig. 1B). After the reaction time, the reactors were cooled and opened at room temperature and the components of the second reaction step were added to the medium (Fig. 1C). Then, urea (10 g) was added to each reactor and manually stirred until the complete dissolution was observed. After that, phosphoric acid (660 µL) was added (the measured pH of the solution was about 2.5). Finally, the MRF sample, previously cut to the dimensions of the ASTM-D 6413:08, was added. Each MRF sample had a mass of approximately 7.1 g ± 1.5; therefore, the ratio of fabric mass to bath volume (RB) was 1:14 (g: mL). The reactors were closed and installed again at HT ALT-I equipment. The reaction was carried out at 130 °C for 2 h with a rotation speed of 40 RPM. After reaction time, the reactors were cooled and opened (the pH of the medium was measured and revealed values between 8.0 and 9.0). The functionalized fabric samples were removed from the medium and fixed in a needled support of the laboratory Stenter LTE-S (Mathis) and were subjected to a drying-cure at 150 °C for 5 min. Afterward, treated samples were reserved in a dry environment at room temperature. Fig. 2 illustrates a proposal for the chemical arrangement after fabric functionalization. The chemical reactions were also studied, and a proposed reaction mechanism is shown in the Supplementary Information.

2.3. Characterization

The morphology of treated fabric samples (T1 and T2) was characterized by SEM-FEG using a JSM-6701F (Jeol) equipment with an EDS

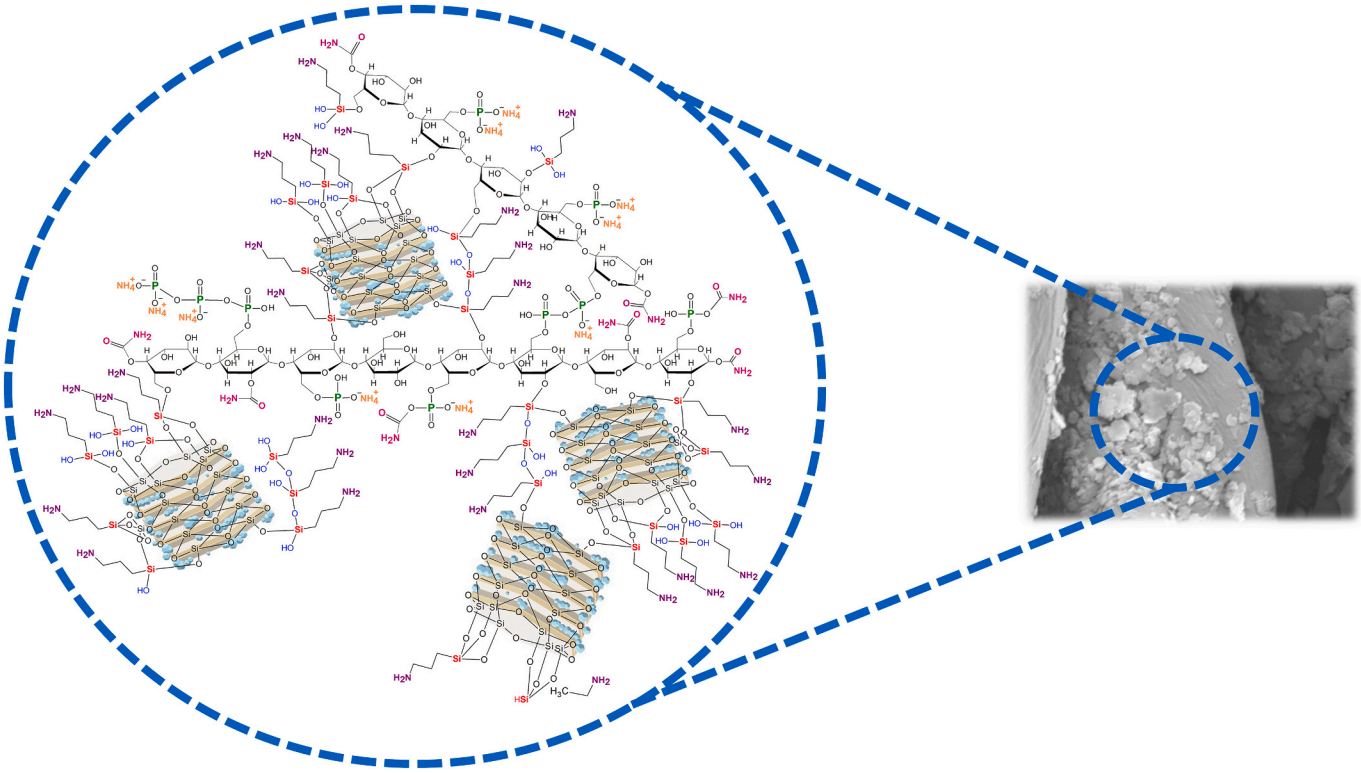

Fig. 2. Proposed schematic illustration of how the components of the finishing formulation adhere to the fiber. The illustration assumes that the silanizing agent acts as a bridge that links the organic (fiber) and inorganic (minerals) phases through the reactive sites, as well as the phosphorus and nitrogen compounds that bind to the unoccupied cellulose hydroxyl sites.

NanoTrace™ X-ray detector (Thermo Scientific) device. The BRF and MRF samples were analyzed by SEM using a TM3030 (Hitachi) equipment.

Thermal behavior of samples was investigated by TGA using a Jupiter STA-449 F3 (Netzsch Germany) equipment; the samples were heated from room temperature to 800 °C with a heating rate of 10 °C·min^{-1} under synthetic air atmosphere, with a flow rate of 20 mL·min^{-1}, and under N_2 flow of 60 mL·min^{-1}.

PCFC (Pyrolysis-Combustion Flow Calorimetry) tests were carried out using the FTT Micro-calorimeter (FTT - Fire Testing Technology Ltd.) equipment. According to ASTM 7309-07, samples were heated from room temperature to 750 °C, with a heating rate of 1 °C·s^{-1}, under nitrogen atmosphere in the pyrolysis chamber, and combustion chamber at 900 °C with a flow rate of N_2 and O_2 at 80 and 20 cc·min^{-1}, respectively.

The FTIR was obtained by Fourier Transform Infrared Spectrum in ATR mode using a CARY 600 - Series FT-IR Spectrometer (Agilent Technologies) equipment, with readings in the region of 4000–400 cm^{-1} with a resolution of 2 cm^{-1}.

The surface charges of MRF, T1, and T2 were also investigated by Zeta Potential using a SurPASS 2 (Anton-Paar) equipment. For all analyses, the samples were tested in duplicate at room temperature (~25 °C) using milli-Q water with a pH range of about 3.5 to about 9.

Vertical burning tests of the fabric samples were based on the ASTM-D 6413:2008 standard. For the test, the fabric samples were prepared in dimensions 30 cm × 7.6 cm and exposed vertically to direct contact with the flame of a Bunsen burner for 12 s. The burning time of each sample was measured until the complete extinction of the flame and after the test the carbonized length was measured.

The determination of the ash content of the fabric samples was adapted from the ABNT NBR 10331:2015 standard. Fabric samples of about 1 g were cut and inserted in porcelain crucibles. The crucibles containing the samples were inserted into a muffle and kept at 800 °C for 2 h. After the test, the residues were weighed to determine the ash content.

The washing resistance test of the treated fabric samples was based on NBR ISO 105-C06:2010 standard. An AATCC:1993 standard WOB (Without Optical Brightener) powder detergent solution of 4 g·L^{-1} in distilled water was prepared. The test was performed in duplicate using HT ALT-I (Mathis) equipment. For the test, 100 mL of the detergent solution, and the fabric sample (T1 and T2) were added in individual containers. The containers were kept under stirring at 40 RPM for 20 min at room temperature. For rinsing, the samples were separately immersed in a beaker containing 100 mL of tap water; and shaken with a glass stick for 1 min. Finally, the samples were subjected to hydro extraction in a bench Padder-Foulard FVH (Mathis) with a pressure of 2 bar and speed of 1 m·min^{-1} and left to dry in an oven at 40 °C.

The tensile strength test was based on the ABNT NBR ISO 13934-1:2016 standard using a Texturometer TA.HD Plus (Stable Micro Systems) equipment and the Exponent Connect Software to records the breaking load values. The test was performed using a 50 kgf load cell (0.5 kN) and a stretching speed of 3 mm·s^{-1} (see results in Supporting Information).

3. Results and discussion

3.1. SEM-FEG analyses

Fig. 3 shows the SEM images of the untreated and treated cotton fabric. Morphology of the BRF fibers (Fig. 3A) shown a naturally flattened and twisted appearance, as reported in the literature (Mansikkamäki et al., 2007; Parikh et al., 2006; Yun et al., 2019). The observed twists are related to the degree of cotton maturation and the slightly rough appearance occurs due to disorientation of the cellulose chains that form the primary wall on the surface of the fibers. The surface of MRF fibers (Fig. 3B) was also shown to be rougher with more

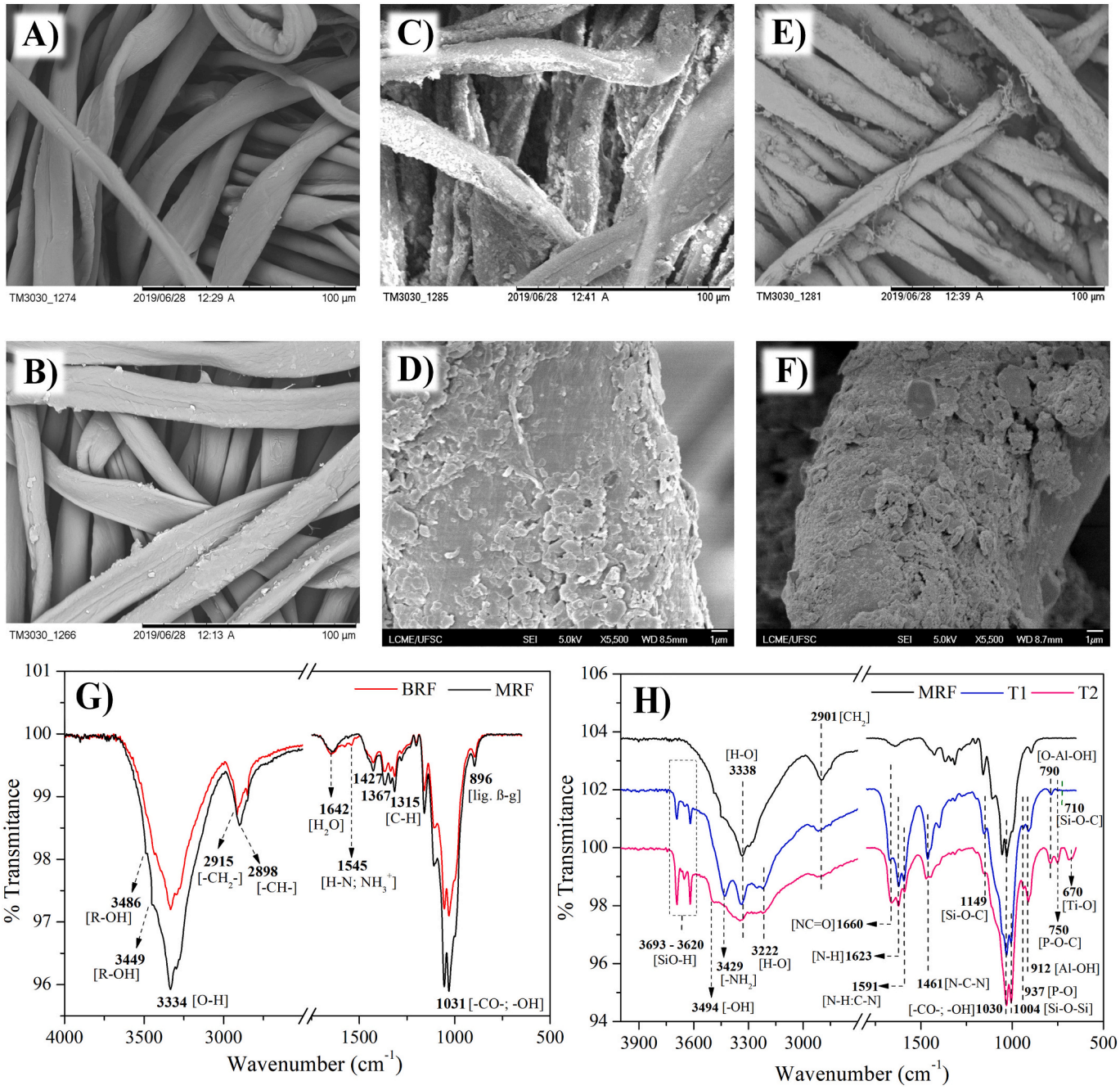

Fig. 3. SEM-FEG micrographs and FTIR analyses of treated and untreated fabric samples: (A) – SEM-FEG of BRF sample; (B) – SEM-FEG of MRF sample; (C)/(D) – SEM-FEG of T1 sample; (E)/(F) – SEM-FEG of T2 sample; (G) – FTIR of BRF and MRF samples, and (H) – FTIR of MRF, T1, and T2 samples.

pronounced grooves, possibly due to the hydrolytic action of NaOH on the primary wall microfibrils (Mansikkamäki et al., 2007; Parikh et al., 2006; Yun et al., 2019). The fibers showed a more cylindrical and linear appearance due to the action of sodium hydroxide (NaOH), which promotes swelling and some changes in the crystalline structure of the fibers with an increase in its porosity.

T1 micrographs (Fig. 3C and D) show a uniform distribution of the micro-nanoparticles (Saleh & Gupta, 2012) onto the surface of the fibers. The images reveal the PK adhered to the fiber-forming a mineral film. T2 micrographs (Fig. 3E and F) also show that the fabric treatment occurred uniformly. The formation of a mineral film with a "dusty" aspect on the fibers; was observed. Furthermore, the fabric structure makes particle diffusion difficult (some fibers uncovered in the background) because it has a closed construction and high grammage. Overall, the images revealed that fabric functionalization was successful for both conditions (T1 and T2).

3.2. *FTIR analyses*

Fig. 3 shows the spectral curves for BRF and MRF (Fig. 3G). Both spectra revealed vibrational modes characteristic of cellulose, such as the intense peak in the 3334 cm^{-1} corresponding to structural hydroxyl groups stretching vibration, and the bands in 2915 cm^{-1} and 2898 cm^{-1} corresponding to the asymmetric and symmetrical stretching of -CH_2- and CH bonds, respectively (De Oliveira et al., 2017, 2021). The absorption band at 1642 cm^{-1} is related to the vibrational deformation of H_2O absorbed in the material, while the bands of 1427 cm^{-1}, 1315 cm^{-1}, and 1367 cm^{-1} are attributed to the vibrational mode of wagging

in the CH bond plane and the axial deformation mode of CH bonds, respectively. The band at 1031 cm^{-1} is characteristic to CO stretching and -OH bonds of cellulose. The peak at 896 cm^{-1} is related to the vibrational way of β-1,4-glucoside stretching bonds outside phase -C1-O-C4- (Allen et al., 2007; Chung et al., 2004; De Oliveira et al., 2017).

In the BRF spectra, a peak at 1545 cm^{-1} unusual for cellulose was observed. According to Mistry (2009), this band is related to the amide stretching and nitrogen groups, which can be attributed to residues of surfactants used in industrial washing or even fabric soiling; this band was not observed after mercerization. MRF spectrum revealed some changes, as the 3486 cm^{-1} and 3449 cm^{-1} which are related to the partial appearance of cellulose II, resulting from the changes caused by mercerization. Such bands correspond to the R-OH bonds vibrational stretching (Saleh, 2011, 2018), which indicate changes in the hydrogen interactions between cellulosic chains after polymorphic transitions, suggesting that an antiparallel arrangement of some cellulose chains was established in the crystalline regions of the fiber (Allen et al., 2007; Kafle et al., 2014; Lee et al., 2013). This effect can be easily observed by increasing the peak intensity at 3334 cm^{-1} band, concerning the same band in the BRF sample (Albinante et al., 2013).

Fig. 3H shows the FTIR spectra of the overlapping MRF, T1, and T2 samples. Between the spectra of T1 and T2, it is also possible to notice some similarities due to the presence of kaolinite and the other components of functionalization, except for the TiO_2 that appears only in T2. Characteristic peaks of cellulose in the region of 3338 cm^{-1} and 1030 cm^{-1} corresponding to O—H bonds vibrational stretching and bonds of the type C—O and -OH respectively, appear in all samples. For samples T1 and T2, absorption peaks were observed in the 3693 cm^{-1}, 3652 cm^{-1}, and 3620 cm^{-1} bands related to the vibrational stretching of silanol (Si-OH) bonds that may come from the kaolinite particle or APTES. Anyway, the appearance of these bands in the fabric reveals the presence of these compounds in the fiber. Absorption band in 3222 cm^{-1} of OH bonds corresponds to the changes in hydrogen bonds intra and interchain after the fiber treatment (Kottegoda et al., 2015; Li et al., 2018; Ratajczak et al., 2015).

The absorption band at 1461 cm^{-1} corresponds to -C-N bonds vibrational stretching, possibly from the APTES free molecule-ends. The absorption peak at 1660 cm^{-1} corresponds to C═O bonds vibrational stretching of NC═O, coming from the cellulose carbamylation by the reaction with the urea decomposition products. The absorption at 1623 cm^{-1} can be attributed to the N—H vibrational deformation (APTES primary amine group). The 1590 cm^{-1} band related to stretching vibration of the primary amine N—H and C—N bond indicates that nitrogen functional groups have been successfully introduced to the cellulose structure (Shuo Huang et al., 2019; Passauer & Bender, 2017; Ratajczak et al., 2015). The absorption peak at 1149 cm^{-1} corresponds to Si-O-C bonds vibration, attributed to bridges formed between the fiber carbon and the silicon of particle, proving the connection between the phases (organic-inorganic). At 710 cm^{-1}, absorption corresponds to the vibrational elongation of Si-OC bonds, typical of the bonds between silicon and carbon by the oxygen of a hydroxyl group. The presence of this band confirms the reaction between cellulose and APTES (Ratajczak et al., 2015). The 790 cm^{-1} absorption band attributed to aluminol bonding vibration (O-Al-OH) indicates the presence of kaolinite particles in samples T1 and T2 (Jose et al., 2019; Li et al., 2018; Parvinzadeh Gashti et al., 2013).

The absorption peak at 937 cm^{-1} corresponds to P-OH vibrational stretching shows the presence of phosphoric groups in the fiber, while the absorption peak in the 750 cm^{-1} refers to P-O-C bonds vibration, indicating that partial phosphorylation of cellulose occurred during the particle embedding reaction (Huang et al., 2019; Suflet et al., 2006; Zhao, 2010). The 670 cm^{-1} absorption band is related to the stretching of the Ti—O bond (Saleh, 2018), in this case belonging to titania incorporated in kaolinite (composite KT applied to T2) (Dědková et al., 2014; Kibanova et al., 2009; Wang et al., 2011).

3.3. TGA-DTG analyses

The results of the TGA analysis of the MRF, T1, and T2 samples under synthetic air flow are shown in Fig. 4A. In this case, during the heating process, up to about 300 °C (first pyrolysis stage), some physical-chemical changes occur in the cotton fiber, accompanied by small mass loss, attributed to dehydration and the beginning of the release of pyrolysis gases. The MRF sample thermogram reveals a small initial mass loss of around 4.8% between room temperature and 110 °C, which can be related to cellulose dehydration. The major degradation step (second pyrolysis stage) occurs between 300 °C and 350 °C with a peak at 334 °C. In this range, thermal degradation occurs, shown by the rapid and intense mass loss of about 65.4%. In this step, most pyrolysis products are produced, such as tar, L-glucose, ketones, alcohols, aldehydes, esters, CO, and H_2O (Moltó et al., 2005). Between 380 °C and 500 °C, there is a significant mass loss (about 27%) related to the char decomposition previously formed; in this phase, there is a high production of aromatic volatiles, such as toluene, benzenes, and phenols (Moltó et al., 2005). From this point on, the following temperatures start char pyrolysis (third pyrolysis stage). Above 500 °C, dehydration and carbonization reactions compete with the L-glucose formation. Mass decomposition is continuous, slower, and more stable; the char continues to dehydrate and decarboxylate, releasing carbonyl and carboxyl products in addition to H_2O and CO_2. With increasing temperature, the remaining carbon content increases (from decomposition products), forming the charred residues. Finally, about 97.3% of the material is degraded at 800 °C, leaving only ash, oxides, and carbonaceous residues.

Degradation temperature displacement of samples T1 and T2 to values lower than the MRF is noticeable. The T1 and T2 thermograms revealed a degradation process in stages, which can be related to the additives present. The T1 thermogram shows an initial mass loss of about 5.2% between room temperature and 236 °C; in this range, the mass loss is related to the cellulose dehydration and the release of volatile products from pyrolysis. DTG analysis (Fig. 4B) revealed a peak at about 176 °C; this peak corresponds to the decomposition of urea carbamates (nitrogen compounds derived from urea contained in the fabric; see Fig. S1). Considering the formulation components applied in T1, this step can be attributed to the decomposition of urea and its derivatives (carbamates) when heated rapidly to above its melting point of about 130 °C (Abushammala, 2019; Harlin, 2019; Passauer & Bender, 2017).

Between 140 °C and 160 °C, urea and/or derivatives becomes liquid, and in the presence of phosphorus compounds, liquefied nitrogen compounds act as a solvent medium for these species and help in the formation of orthophosphate and ammonium pyrophosphate, which occurs close to 200 °C. With additional heating, another species emerge from the decomposition of orthophosphate and pyrophosphate, such as orthophosphate ester and ammonium metaphosphate (Nam et al., 2012). This step can be seen in the T2 thermogram, which occurs between 120 °C and 180 °C (peak at 167 °C) with a mass loss of about 9.9%.

For T1 and T2, a degradation step between 220 °C and 310 °C, with peaks at 282 °C and 283 °C, and mass loss of 33.7% and 37.8%, respectively, was observed. For both samples, after the degradation peak of cellulose, it is observed that a smaller and continuous mass loss occurs between 350 °C and 700 °C. Within this range, some events can occur up to about 450 °C, as the degradation of organic matter; in this case, the most likely would be the APTES decomposition that involves the incorporated PK and KT particles. There may also be structural water loss from the PK particle's edges. Between 500 °C and 700 °C, in this case, crystalline structural changes in the particles occur; at these temperatures, the kaolinite undergoes dehydroxylation (loss of hydroxyls) and gives rise to metakaolinite (Ribeiro et al., 2018).

For Gaan and Sun (2007a), the presence of phosphoric acid and its derivatives leads to a catalyzed cellulose degradation on the fiber surface, which causes the fiber's degradation temperature to shift to lower values. They found that cotton fabrics treated with phosphoric acid have

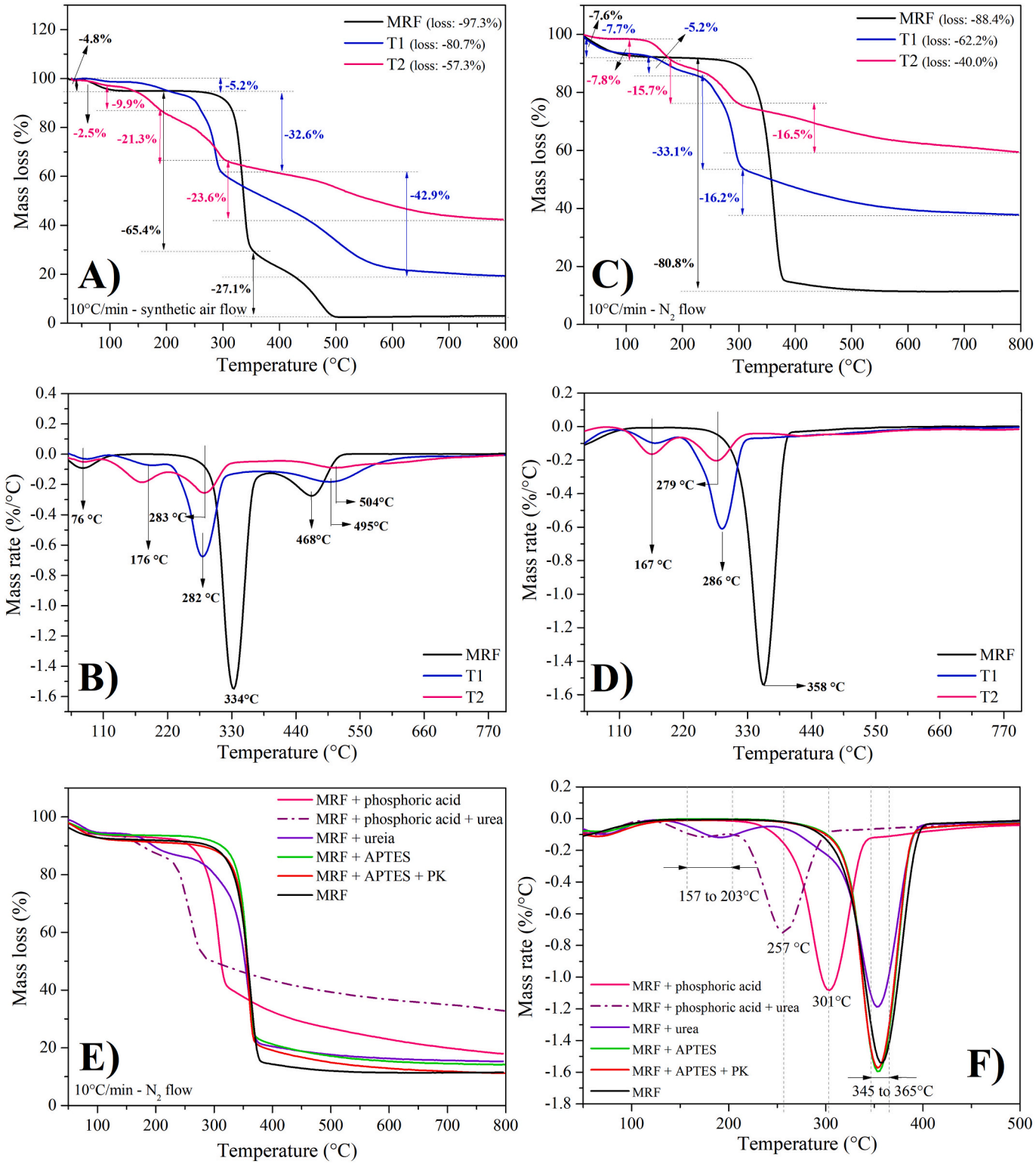

Fig. 4. TGA-DTG analyses: (A) – TGA curves of MRF, T1, and T2 samples under synthetic air atmosphere; (B) – DTG of MRF, T1, and T2 samples under synthetic air atmosphere; (C) – TGA curves of MRF, T1, and T2 samples under N_2 atmosphere; (D) – DTG of MRF, T1, and T2 samples under N_2 atmosphere; (E) - TGA curves of the formulation components applied alone to the fabric, and (F) - DTG of the formulation components applied alone to the fabric.

higher activation energy (E_a) (214 kJ·mol^{-1}) than the E_a of untreated fabrics (150 kJ·mol^{-1}) (Gaan & Sun, 2007b). According the authors, the increase in E_a of the fabric gives it an increase in its thermal stability between 200 °C and 400 °C. Protective layer formation can also be related to the mineral particles incorporated since they similarly act in the condensed phase.

Larger amounts of carbonaceous residues at the final may indicate a reduction in the flammability of the fiber. TGA analysis under synthetic air flow showed that at 800 °C, the MRF sample had a mass loss of about 97%, while T1 and T2 had a mass loss of 80% and 57%, respectively. These results show the effectiveness of treatments in the thermal protection of cotton fibers. It is also notable the difference in the residues

contained in the T2 sample concerning T1. Considering that the treatment procedure is similar for T1 and T2 samples, except for the difference between the particles used (PK and KT); possibly, the improvement in the thermal behavior of the T2 concerning T1 is related to the presence of titania. For comparison, the TGA-DTG tests were also conducted under an N_2 atmosphere. The main degradation phases of the fabric samples (treated and untreated) were observed (Fig. 4C), and the same thermal events that occur under synthetic air also occur under N_2 at similar temperatures (Fig. 4D). The most relevant difference is in the greater mass degradation of the samples under the synthetic air atmosphere. It occurs due to the oxygen present, which makes the test atmosphere much more oxidative (reactive) concerning the N_2 atmosphere (inert).

Following the same reaction conditions (time, temperature, and concentration), as reported in the experimental procedure (see Section 2.2.3), the formulation components were applied alone to the fabric. Then, the same thermal evaluations on the prepared samples; were made. These tests, allowing to visualize the effect that each component has on the fiber's degradation and heat release. We observed that, except for phosphoric acid and its combination with urea, no other component showed a relevant reduction in mass degradation and heat released (see Fig. 5B) from the tested cotton fabric. Even for samples treated only with phosphoric acid or its combination with urea (best results among the other components applied alone), their results are not similar to T1 and

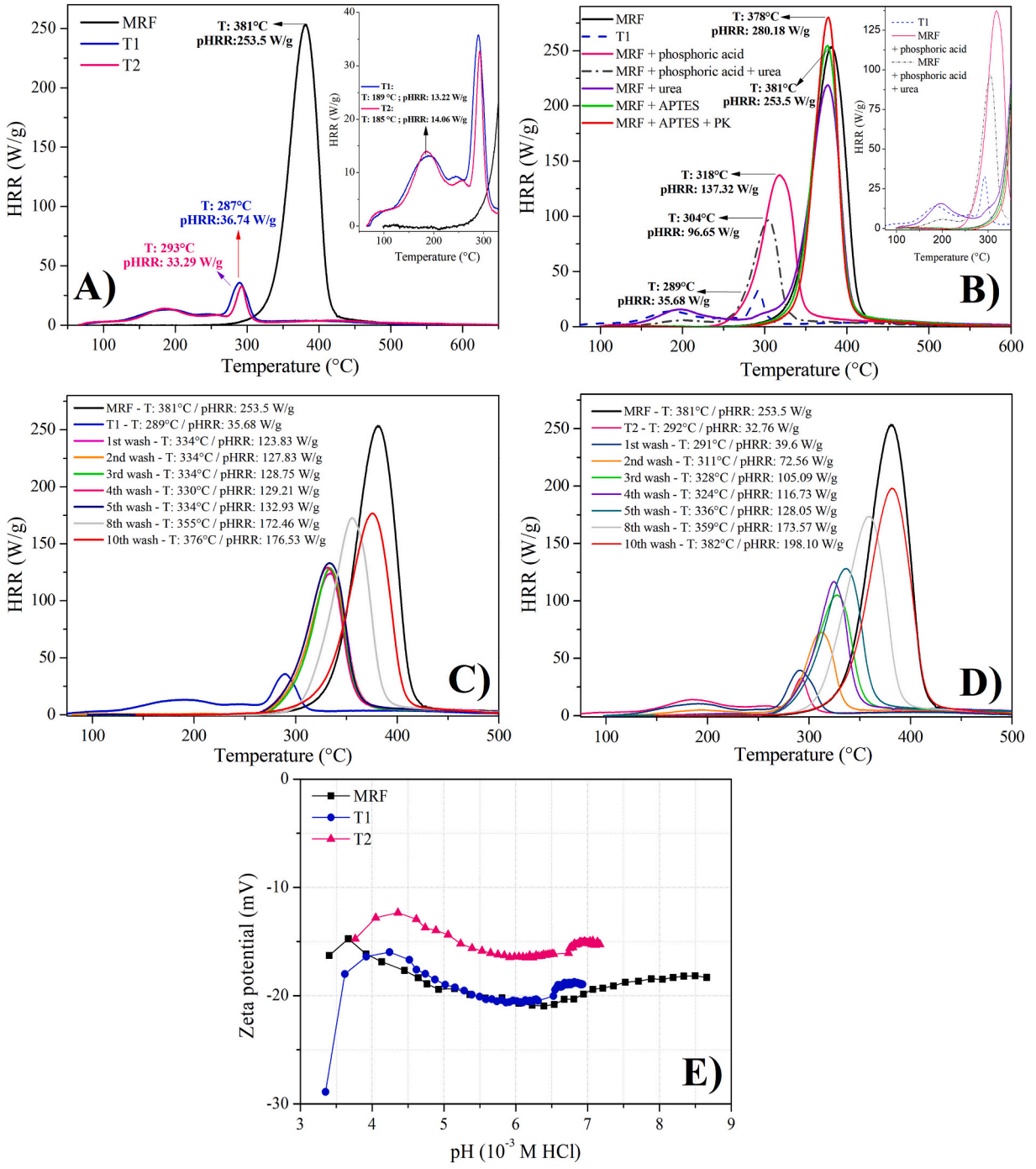

Fig. 5. PCFC and Zeta Potential analyses: (A) - PCFC analyses of MRF, T1, and T2 samples; (B) – PCFC analyses of the formulation components applied alone to the fabric; (C) - PCFC of T1 samples after washes; (D) - PCFC of T2 samples after washes, and (E) – Zeta Potential analyses of MRF, T1, and T2 samples.

T2 samples that contain PK and KT, respectively (see Fig. 4E and F). Therefore, the presence of kaolinite and the composite in the fabric is of great relevance; for the self-extinguishing behavior observed in the vertical burning test; the high resistance to degradation and residue formation observed in the TGA analyses, and the low heat release revealed in the PCFC.

3.4. PCFC analyses

The PCFC (Pyrolysis-Combustion Flow Calorimeter) analysis verifies the amount of heat released from a material during its pyrolysis. To measure the heat released, the PCFC correlates the oxygen consumption necessary to oxidation of combustible gases released by pyrolysis. Fig. 5A shows the PCFC results of the MRF, T1, and T2 samples. The MRF sample showed a pHRR of 253.50 $W \cdot g^{-1}$ and a decomposition temperature of about 381 °C. This result corroborates the thermal degradation temperature of cellulose observed by TGA, which occurs between 300 °C and 400 °C. For both T1 and T2, we observed that the release of volatile products occurs in two stages. The first minor step occurred between 130 °C and 250 °C. In this range, the heat released could be related to the release of some urea derivatives or carbamates (explained in Fig. S1) from the main cellulose chain, with the possible release of low calorific volatile compounds (Liang et al., 2012), which was also observed in the TGA analyses.

In this stage, there is also the release of some primary pyrolysis compounds of cellulose. Between 270 °C and 320 °C, the maximum degradation of samples T1 and T2 occurs; this second stage, being the most energetic, is marked by the release of high calorific decomposition products. The treated fabric samples exhibited a remarkable decrease in pHRR and THR. The treatment of fabrics chemically promoted, in the condensed phase, the formation of thermally stable compounds and raised char residue of cotton. The treatment of fibers may have accelerated the production of char. Thus the more organic matter was catalytically carbonized during the charring process instead of being transferred into combustible volatile compounds (Cheng et al., 2020); This fact corroborates the higher final mass observed in the TGA tests.

This behavior explains the low rate of heat release from T1 (36.74 $W \cdot g^{-1}$) and T2 (33.29 $W \cdot g^{-1}$); since it is calculated by the oxygen consumption necessary to burn the volatiles released by the samples. In general, the results showed a reduction of more than 85% in the heat release peaks (pHRR) for the T1 and T2 samples compared to MRF (see Table 1). The higher formation of residues by T1 and T2 contributes to the total heat released (THR) reduction compared to MRF due to the lower release of volatile fuels. This phenomenon was also observed in the TGA analyses, and the same thermal events revealed by DTG (see Fig. 4B and D) were observed in the PCFC data.

Table 1
Data obtained from the PCFC for the MRF, T1 and T2 samples.

Sample	pHRR[a] ($W \cdot g^{-1}$)	T_{pHRR}[b] (°C)	Reduction in pHRR (%)[c]	THR[d] ($kJ \cdot g^{-1}$)	Char yield (%)[e]
MRF	253.50 ± 0.00	381 ± 0.00	–	12.86 ± 0.00	13.75 ± 0.00
T1	36.74 ± 1.50	287 ± 2.83	85.51 ± 0.59	3.16 ± 0.05	38.77 ± 0.22
T2	33.29 ± 0.75	293 ± 1.41	86.87 ± 0.30	2.93 ± 0.03	54.06 ± 2.92

[a] Peak heat release rate.
[b] Temperature of peak heat release rate.
[c] % reduction of T1 and T2 peak concerning to the MRF sample.
[d] Total heat released.
[e] % of residue at the final of the analysis. (Note: Results are reported as "mean ± standard deviation" from two independent determinations).

3.5. Zeta potential analyses

The dyeing ability, visual appearance, effectiveness of finishing operations, and usability are strongly related to the properties of the fabric surface. Therefore, changes in the textile surface caused by physical-chemical finishes, such as the immobilization of particles on the fibers, can substantially alter the material properties, so they need to be understood (Grancaric et al., 2005; Ripoll et al., 2012). The surface charge of fabrics is related to the dissociation of chemical groups on their surface, such as hydroxy and carboxy groups. Therefore, the charge may suggest differences in the availability of reactive sites. Even as changes in fiber hydrophilicity and hydrophobicity (Ripoll et al., 2012). For the above reasons, samples of the treated and untreated fabric have been investigating by the Zeta Potential technique.

To study the electrokinetic properties of treated and untreated samples surface, the Zeta Potential for MRF, T1, and T2, was measured individually. Fig. 5E shows the results of each of the analyzed samples. For MRF, results showed negative Zeta Potential values, between −15 mV and −20 mV for the pH range between 3.0 and 9.0, according to the results found in the literature (Ripoll et al., 2012). The electronegativity of the textile surface of MRF is related to its high hydrophilicity and reactive potential through the hydroxyl groups of pure cellulose. Pure cotton fibers contain many hydroxyl and carboxyl-type groups on their surface, which explains their excellent absorption capacity and high hydrophilicity, especially in the case of a mercerized material, as it presents greater porosity and availability of these groups in the fiber (Grancaric et al., 2005; Luxbacher, 2014). In this analysis, the isoelectric point (IEP) was not found. Many authors report the IEP of the raw cotton fabric for pH values $\leq$ 2.5 (Grancaric et al., 2005; Luxbacher, 2014; Ripoll et al., 2012). However, we conducted the analyses in the pH range between 3.5 and 9.0. In this range, results are reliable concerning the sensitivity limitations of the equipment. Outside this range, the ionic strength varies significantly with the pH, which at very low values reduces the magnitude of the measured Zeta Potential.

The T1 and T2 curves also showed negative Zeta Potential values for the entire pH range tested, except for the difference of −10 mV between the points of the curves along of pH range. The T1 result proved to be closer to MRF than to T2, possibly, due to the presence of TiO_2 in T2, which causes possible changes in the electrokinetic behavior of the fabric. Despite the particles immobilized in the fibers, their presence in the fabric causes little change in the charge profile of the material surface. Samples T1 and T2 did not show alterations in surface charge over the tested pH range. This characteristic reveals that T1 and T2 are highly hydrophilic. Possibly, due to a large amount of hydroxyl, carboxyl, carbonyl, and other polar groups, belonging not only to cellulose but also to the incorporated additives (*e.g.,* PK and KT). Therefore, it can be expected that the treated fabric has excellent absorption (in fiber) and adsorption (in minerals) capacities due to the high availability of reactive surface sites.

3.6. Vertical burning tests of untreated and treated cotton fabric

Table 2 presents the vertical burning results for the MRF, T1, and T2 samples. The MRF sample showed total burning (30 cm = sample size) as expected since the fabric does not have any retardant treatment applied. The time for the complete burning of the MRF samples is about 72 s, which provides a rate of 3.15 $cm^2 \cdot s^{-1}$. When T1 and T2 are exposed to flames in a Bunsen burner, they present slow degradation without ignition, *i.e.*, only a process of localized latent pyrolysis occurs during the exposure for both conditions. When the contact with flames is removed, occurs an instant interruption of the decomposition. Therefore, no formation and propagation of fire was observed in the treated samples, as shown in Fig. 6. The carbonized length (length of the area directly exposed to the flame) for T1 and T2 was about 3.7 cm and 3.2 cm, respectively.

Fig. 7 shows the micrographs of the charred region of MRF, T1, and

Table 2
Results of the vertical burning test of the treated samples before and after the washes in comparison to the mass values of the samples.

Sample	C. L.[a] (cm)	B. T.[b] (s)	Gm.[c] ($g \cdot m^{-2}$)	M. L. F.[d] (%)	B. S.[e] ($cm^2 \cdot s^{-1}$)
MRF[f]	Complete burning	72.00 ± 2.00	314 ± 1.85	–	3.15
T1	3.70 ± 0.40	No flame spread	444.81 ± 8.72	–	–
T1: 1st wash	9,60 ± 0.40	No flame spread	404.70 ± 7.07	30.66 ± 0.78	–
T1: 3rd wash	30.00 ± 0.00	44.00 ± 2.00	394.74 ± 5.61	38.28 ± 1.31	5.18
T1: 5th wash	Complete char formation	46.00 ± 3.00	390.13 ± 1.55	41.80 ± 1.08	4.96
T1: 10th wash	Complete char formation	56.00 ± 2.00	337.86 ± 2.06	81.76 ± 0.61	4.07
T2	3.20 ± 0.30	No flame spread	464.66 ± 1.72	–	–
T2: 1st wash	7.80 ± 0.60	No flame spread	434.40 ± 1.51	20.09 ± 1.59	–
T2: 3rd wash	30.00 ± 0.00	55.00 ± 2.00	393.04 ± 3.36	47.53 ± 0.38	4.15
T2: 5th wash	Complete char formation	48.00 ± 2.00	388.86 ± 0.59	50.31 ± 1.39	4.75
T2: 10th wash	Complete char formation	52.00 ± 3.00	348.81 ± 2.11	76.89 ± 0.82	4.38

[a] Carbonized length.
[b] Burning time.
[c] Grammage of samples.
[d] Mass loss of finishing.
[e] Burning speed.
[f] Mercerized raw fabric. (Note: Results are reported as "mean ± standard deviation" from two independent determinations).

T2 after the vertical burning resistance test. It is interesting to note that, unlike the MRF sample, T1 and T2 samples showed higher fiber preservation after the test. Fig. 7A and B shows that the fibers have undergone higher degradation, as they appear broken. It is possible to notice that in Fig. 7C and D of T1 and in Fig. 7E and F of T2, even after burning, it keeps the presence of PK and KT particles incorporated into the fiber.

Two competing reactions determine the final state of biopolymer degradation during the cellulose pyrolysis (Egyed & Simon, 1979; Hajj et al., 2020; Horrocks, 1983). One of them is the cellulose degradation reaction that forms char, and the other is related to the molecular scission reactions in the main chain that leads to the formation of molecular species of low molecular weight, and therefore volatile as well as highly flammable (Gaan & Sun, 2007a; Hajj et al., 2020; Horrocks, 1983). In this case, volatile fuel species are oxidized by oxygen in the air (Horrocks, 1983). The oxidation reaction of these species is exothermic, and the region where these phenomena occur has a constant increase in temperature, and therefore a progressive release of heat. The temperature rise feeds the cellulose pyrolysis process, which releases more combustible gaseous compounds, and the continuation of the reactions starts the ignition. From that moment, the flame propagates and accelerates these reactions until the complete degradation. For the treated fabric, during combustion, phosphorus groups are decomposed, releasing acidic molecules, such as phosphoric acid, which catalyzes cellulose dehydration and promotes the formation of char instead of volatile combustible species (Hajj et al., 2020).

As described in the literature, the mode of action of metal oxides, nanoclays, clay minerals, organophilic clays, and siloxanes is limited to the solid phase. These compounds form a protective mineral layer over the burning materials. This layer promotes thermal insulation, limiting the diffusion of pyrolysis gases out of the substrate, and protecting the sample from irradiated heat, as illustrated in Fig. 7K (Dasari et al., 2013; Kiliaris & Papaspyrides, 2010; Laoutid et al., 2009). Phosphorus and nitrogen compounds act mainly in the condensed phase by the phosphorylation of the cellulose. They may also operate in the gas phase by a radical trapping mechanism and by combustible gas dilution.

Nam et al. (2012) studied the synergistic effects of urea with a phosphorus compound, with different concentrations, through the E_a measures of the FRs on treated and untreated fabric. They found that for a fixed amount of phosphorus compound, the amount of urea directly interferes with the temperature of cotton degradation; besides that, the components, when applied alone, do not show significant fireproof. The authors reported that the FRs (composed of phosphorus and urea) usually have the E_a lower than the E_a of cotton fabric without treatment, and therefore the decomposition point of these FRs is far below the cellulose degradation temperature. It explains the shift in the degradation temperature of T1 and T2 to lower temperatures, observed in the TGA and PCFC since the decomposition of these compounds generates products that accelerate the superficial degradation of the fibers and promote the formation of char. During the beginning of heating, liquefied urea permeates the amorphous regions of the fiber and opens the way for the entrance of phosphorous compounds. In the beginning, urea improves the intermolecular permeability of fibers in the fabric. In this way, the transfer of heat and mass (pyrolysis gases) is facilitated, such as the permeability of the additives applied to the fibers. These phenomena accelerate the surface decomposition of fibers, which occurs at slightly lower temperatures. As the heating progresses, the reactions between urea and the phosphorus compound inside the fibers promote their phosphorylation. The pyrolysis reactions continue, and the cellulose decomposition products with the FRs combine, forming the carbonaceous layer. Therefore, the degradation tends to stop because the E_a of the carbonized fabric is much higher.

3.7. EDS analyses

The EDS analysis of the carbonized length residues of the samples after the vertical burning test (Fig. 7I and J) showed the remaining presence of all the elements of the applied formulation, which indicates that the flame retardancy phenomena in this type of finish occur mostly in the solid phase, through the interaction between the components of the formulation and the fiber with the formation of a carbon-mineral layer (see Table S1). The content of "N" does not change much in the proportions found in the residue, which indicates that a small part is volatilized and acts in the gas phase, while the majority remains in the char. The proportions of "C" increase substantially due to the formation of char, while the "O" decreases due to the dehydroxylation of cellulose and volatilization in the form of low molecular weight organic species. As expected, the proportions of "Si", "Al" and "Ti" slightly increase in the mass of the residue due to the redistribution of the proportions of the remaining components that occupy the mass value of the volatilized elements during pyrolysis. The increase of "P" in the residue indicates that for this treatment type, phosphorus in pyrolysis/combustion acts in the solid phase, promoting the formation of a stable glassy and charred protective layer that contributes to the extinguishing of fire and/or the non-propagation of flames (Lopez-Cuesta, 2017; Morgan & Wilkie, 2007).

3.8. Ash content determination test of untreated and treated cotton fabric

The ash content analysis allows the verification of the inorganic material content present in an organic matrix. In this test, the high temperature decomposes the organic materials in the sample, leaving only the minerals, metallic oxides, and other inorganic substances that compose the ashes. Fig. 8 shows the images of the calcination residues of the muffle furnace for the MRF, T1, and T2 samples. Fig. 8I shows the MRF residue, which presented the content of 0.18% ± 0.021 of mass concerning the initial weight (1 g). In this case, only the ashes remained in the residue (salts, metal hydroxides, oxides, and minerals like sodium, calcium, and others). In Fig. 8J, the T1 sample appears dark, indicating the formation of a char. The aspect of the calcined samples is related to the carbonaceous layer. The residual content of 9.14% ± 0.91 confirms

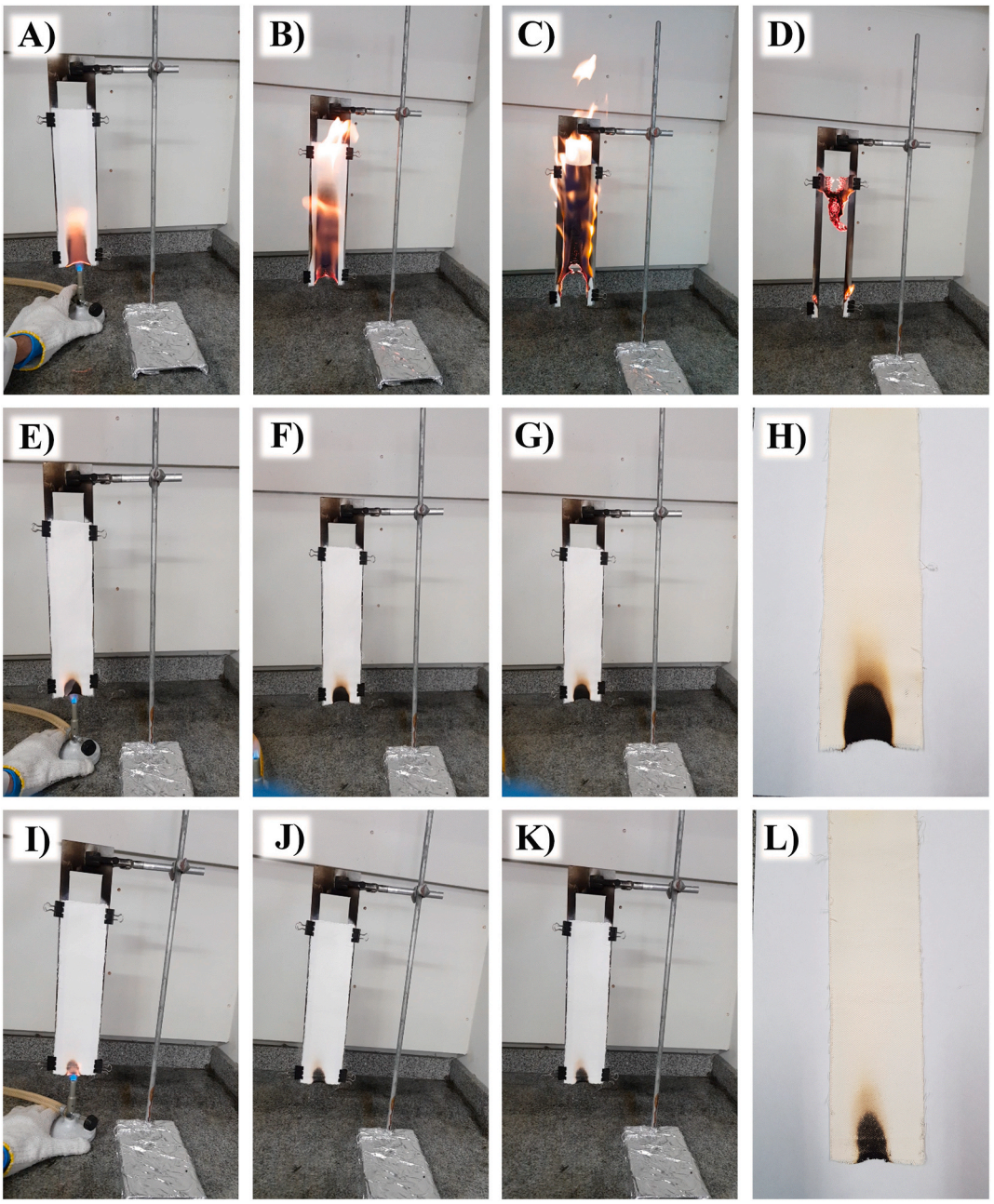

Fig. 6. Pictures of the vertical burning test in progress for the T1 and T2 samples: (A)/(B)/(C)/(D) – Vertical burning test of MRF at times of 12 s, 22 s, 32 s, and 48 s, respectively; (E)/(F)/(G)/(H) – Vertical burning test of T1 at times of 8 s, 12 s, 20 s, and after test, respectively, and (I)/(J)/(K)/(L) – Vertical burning test of T2 at times of 8 s, 12 s, 20 s, and after test, respectively.

that part of the organic matter is preserved. In Fig. 8J and K, there is a visual indication that the silicon compounds present help to form an intumescent and expansive carbonaceous layer on the surface of the fibers. In Fig. 8K the aspect is even more intriguing. A gray tone that covers the fabrics shows the mineral layer formation on the surface of the fibers. The grayish appearance and the puffiness are due to the titania and the clay mineral present in the sample. The content of 11.49% ± 1.72 of final residue shows that the titania causes a thermal reinforcement.

3.9. Washing resistance test of the treated cotton fabric evaluated by PCFC and the vertical burning tests

Fig. 5C shows the PCFC results for the washed T1 samples. After the first five washes, the T1 samples were testing. Thus, it was possible to observe the changes that occur as soon as the fabric starts to be washing. The tests; were also carried out for eight and ten washes. The PCFC curves show that T1 right after the 1st wash has a pHRR much higher; than the value of the unwashed sample, with a significant increase (247%) of heat release. However, a certain constancy in the pHRR value until the 5th wash; can be observed. After the 5th wash, T1 still presents a reduction of 51% of the heat released concerning the MRF. The 8th and 10th washes showed pHRR values higher pHRR than the first five washes, indicating a gradual loss of the retarding effect due to leaching of the particulate components. The pHRR has an increase of 30% approximately in the heat release for the 8th and 10th wash. The results show that the loss of treatment efficiency is progressive, albeit slow until the 5th wash and that the highest loss occurs after the 1st wash.

Fig. 5D shows the PCFC results for the washed T2 samples. The PCFC curves reveal that T2 has no significant increase in heat release after the

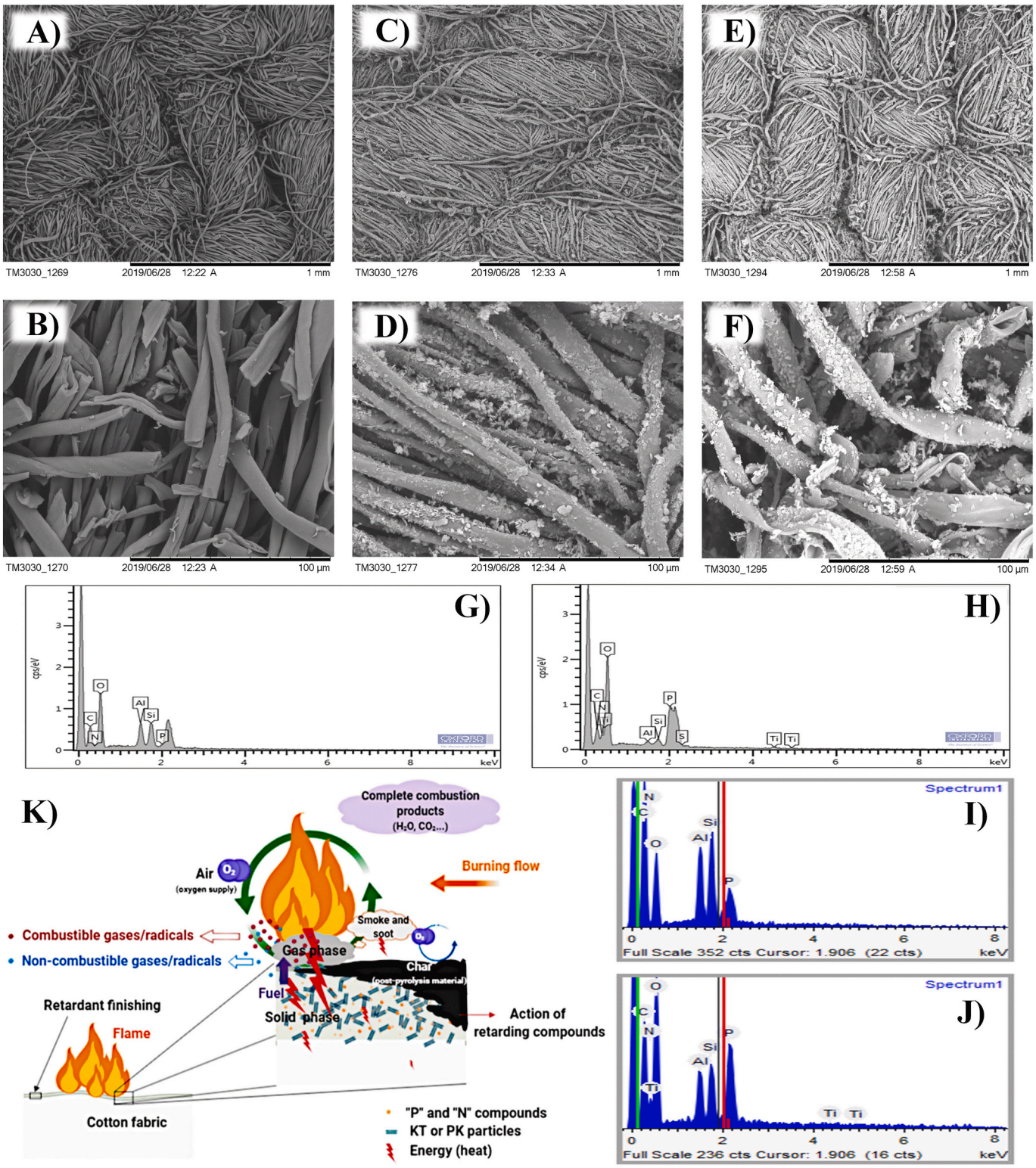

Fig. 7. SEM-FEG micrographs of untreated and treated fabric samples after burning (carbonized length samples after the vertical burn test); EDS analyses of T1 and T2 samples before and after vertical burning test, and combustion mechanism illustration of the functionalized fabric: (A)/(B) – SEM-FEG of burned MRF sample; (C)/(D) – SEM-FEG of burned T1 sample; (E)/(F) – SEM-FEG of burned T2 sample; (G) – EDS analysis of T1 before burning test; (H) - EDS analysis of T2 before burning test; (I) - EDS analysis of T1 after burning test; (J) - EDS analysis of T2 after burning test. (K) - Schematic illustration of the flame retardant mechanism proposed for the finishing applied to the fabric: The contact of the finishing with the heat source promotes the release of species that accelerate the degradation of cellulose on the fabric surface, which occurs at a lower temperature (see TGA analysis). The interaction effects between the applied components catalyze the formation of a carbonaceous layer that together with the minerals present generates a thermal protection barrier of the carbon-mineral type, which hinders the heat exchange and oxygen feedback, reducing the temperature of the system and inhibiting the spread of flames.

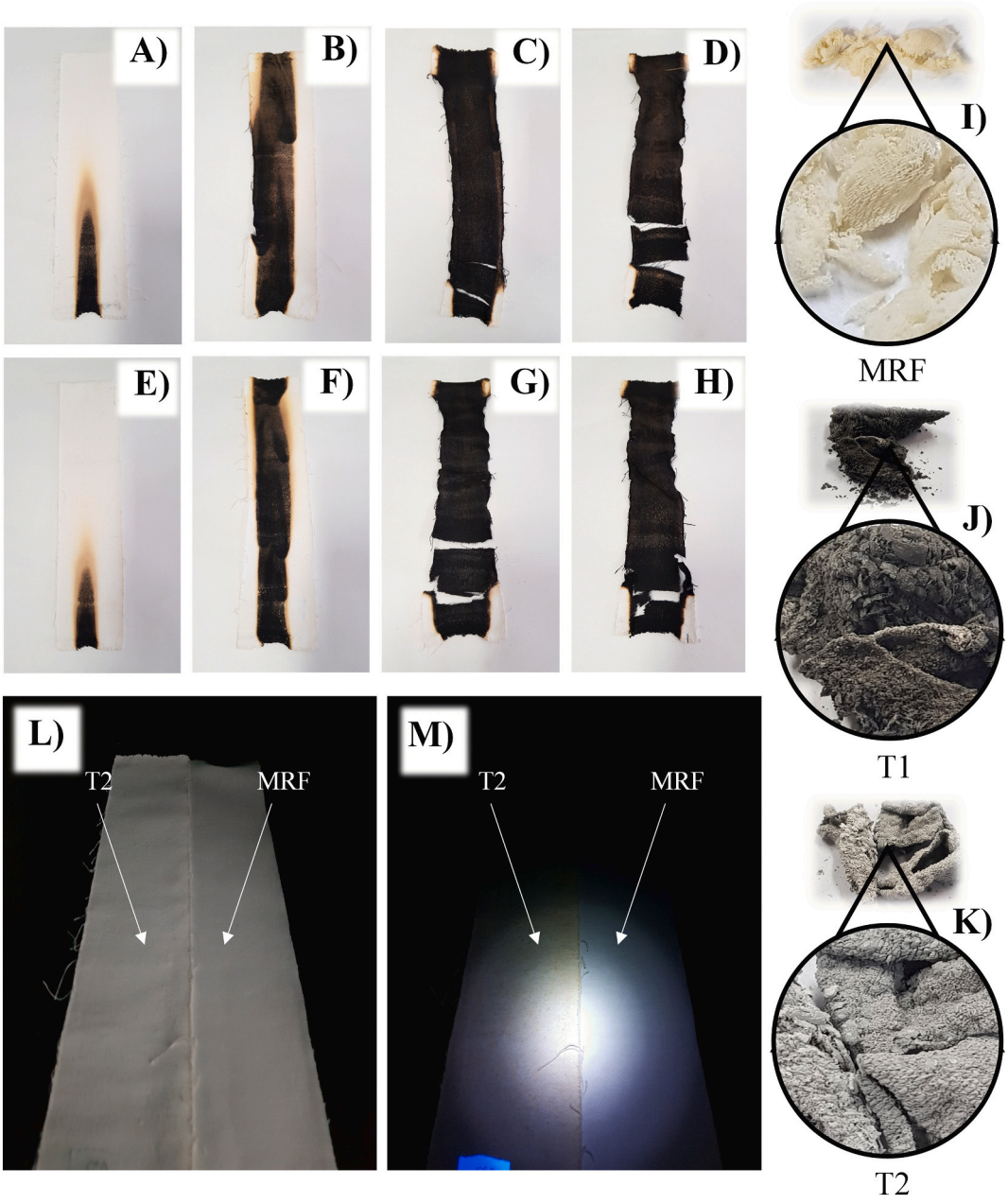

Fig. 8. Pictures after the vertical burning test of the samples previously washed, and pictures of MRF, T1, and T2 residues after the ash determination test: (A)/(B)/(C)/(D) – T1 sample burned after the 1st, 3rd, 5th, and 10th wash, respectively; (E)/(F)/(G)/(H) – T2 sample burned after the 1st, 3rd, 5th, and 10th wash, respectively; (I)/(J)/(K) - Aspect of the MRF, T1, and T2 residues after the ash determination test, respectively; (L) - Sample of T2 (on the left) and MRF (on the right) inside a black chamber in an environment with little natural light (in natural light the presence of minerals on the fabric is barely noticeable), and (M) - Sample of T2 (on the left) and MRF (on the right) inside a black chamber in a dark environment under the illumination of a 390 nm UV LED flashlight (At 390 nm, the presence of minerals in the fabric is quite noticeable).

1st wash. However, after the 5th wash, T2 reaches a pHRR value very similar to that of T1. Therefore, after washing, the amount of leached material of both samples appears to be similar. The results of the 8th wash, between T1 and T2, are resembling, while the 10th wash of T2 has a pHRR value close to that of the MRF. In this case, after the 10th wash, there is no more retarding action on the fabric; all the content of the finishing applied has undergone chemical modifications or has been leaching.

The T1 and T2 samples after the 1st, 3rd, 5th, and 10th washes, were used in the vertical burning test. With that, we observed the burning behavior (retarding effect) of the samples (see Table 2). Reduction of the retarding effect is easily seen with the progression of washes to T1 and T2, possibly, due to the formulation components leaching. During the washing, the water action (with agitation) can induce the loss of some particles that are weakly adhered to the fiber. Chemical changes caused by the action of alkaline cleaning products can cause, for example, the replacement of NH_4^+ ions attached to phosphates by Na^+ ions, decreasing the retarding efficacy promoted by the interaction of phosphorus and nitrogen, among others. Although the results are good even after a few washes (from Fig. 8A to H), they are not satisfactory for applications that require frequent washing; in this case, treatments with crosslinkers can be a possible solution for leaching. For dry applications that do not require washing the material, the treatment shows effective and excellent results.

4. Conclusions

In this study, a kaolinite-TiO_2 (KT) nano-hybrid composite was synthesized. After it, KT composite was incorporated into a cotton fabric using a formulation containing phosphorus and nitrogen compounds. Microscopy analyses showed the excellent coverage of the fibers. Likewise, FTIR analysis showed that the components applied into fabric reacted with the cellulose confirming the fibers functionalization. The TGA and PCFC analyses of the treated samples revealed their high capacity for char formation, suggesting a predominant flame-retardancy mechanism in the solid phase, which we attribute, especially, to the presence of the kaolinite and TiO_2 minerals. TGA and PCFC analyses also showed thermal degradation 41% less for treated fabric concerning the untreated fabric sample at 800 °C and a reduction of about 85% in peak heat release (pHRR). EDS analysis showed the presence of the finishing compounds remaining in the fabric after the burning test, which confirmed the predominance of the flame retardancy phenomenon in the solid phase. We observed excellent fireproof through the vertical burning tests in which the samples exposed to fire showed self-extinguishing behavior after removed from contact with the flame. Compared to the actual methodologies used to flame retard cotton, the present work offers a facile and safe way to prepare fabrics with excellent flame retardant properties from a more sustainable process.

CRediT authorship contribution statement

Carlos Rafael Silva de Oliveira: Conceptualization, Methodology, Validation, Formal analysis, Investigation, Writing – original draft, Writing – review & editing, Visualization, Project administration. **Marcos Antonio Batistella:** Conceptualization, Formal analysis, Writing – review & editing, Supervision. **Selene Maria de Arruda Guelli Ulson de Souza:** Resources, Writing – review & editing, Supervision, Funding acquisition. **Antônio Augusto Ulson de Souza:** Resources, Writing – review & editing, Supervision, Funding acquisition.

Declaration of competing interest

The authors declare that they have no known competing financial interests or personal relationships that could have appeared to influence the work reported in this paper.

Acknowledgments

The authors are grateful to Coordenação de Aperfeiçoamento de Pessoal de Nível Superior (CAPES, Brazil) for the financial support (Finance Code 001) and to the Federal University of Santa Catarina (UFSC), for the structure of its laboratories to this research: Mass Transfer Laboratory (LABSIN-LABMASSA); Central Laboratory of Electronic Microscopy (LCME); Interdisciplinary Laboratory for the Development of Nanostructures (LINDEN); Ceramic and Composite Materials Research Laboratory (CERMAT); Process Control Laboratory (LCP); Glass Ceramic Materials Laboratory (VITROCER) and the Chemical Engineering Analysis Center (CENTRAL-EQA). The authors also grateful the companies IMERYS-Brazil and PARANATEX Têxtil (Brazil) for the donations of kaolinite and the bleached cotton fabric, respectively, used in this work.

Appendix A. Supplementary data

Supplementary data to this article can be found online at https://doi.org/10.1016/j.carbpol.2021.118108.

References

Abushammala, H. (2019). A simple method for the quantification of free isocyanates on the surface of cellulose nanocrystals upon carbamation using toluene diisocyanate. *Surfaces, 2*(2), 444–454. https://doi.org/10.3390/surfaces2020032

Albinante, S. R., Pacheco, É. B. A. V., & Visconte, L. L. Y. (2013). Revisão dos tratamentos químicos da fibra natural para mistura com poliolefinas. *Química Nova, 36*(1), 114–122. https://doi.org/10.1590/S0100-40422013000100021

Ali, N., Harrad, S., Muenhor, D., Neels, H., & Covaci, A. (2011). Analytical characteristics and determination of major novel brominated flame retardants (NBFRs) in indoor dust. *Analytical and Bioanalytical Chemistry, 400*(9), 3073–3083. https://doi.org/10.1007/s00216-011-4966-7

Allen, A., Foulk, J., & Gamble, G. (2007). Preliminary Fourier-transform infrared spectroscopy analysis of cotton trash. *Journal of Cotton Science, 11*(1), 68–74.

Al-Mosawi, A. I., Abdulsada, S. A., Rijab, M. A., & Hashim, A. (2015). Flame retardancy of biopolymer polyhydroxyalkanoate composite. *International Journal of Advanced Research, 3*(8), 883–886. Doi:10.13140/RG.2.1.1465.9282.

Bajaj, P. (1992). Flame retardant materials. *Bulletin of Materials Science, 15*(1), 67–76.

Baydar, G., Ciliz, N., & Mammadov, A. (2015). Life cycle assessment of cotton textile products in Turkey. *Resources, Conservation and Recycling, 104*, 213–223. https://doi.org/10.1016/j.resconrec.2015.08.007

Cheng, X. W., Tang, R. C., Guan, J. P., & Zhou, S. Q. (2020). An eco-friendly and effective flame retardant coating for cotton fabric based on phytic acid doped silica sol approach. *Progress in Organic Coatings, 141*(September 2019), 105539. https://doi.org/10.1016/j.porgcoat.2020.105539

Chung, C., Lee, M., & Choe, E. (2004). Characterization of cotton fabric scouring by FT-IR ATR spectroscopy. *Carbohydrate Polymers, 58*(4), 417–420. https://doi.org/10.1016/j.carbpol.2004.08.005

Dasari, A., Yu, Z. Z., Cai, G. P., & Mai, Y. W. (2013). Recent developments in the fire retardancy of polymeric materials. *Progress in Polymer Science, 38*(9), 1357–1387. https://doi.org/10.1016/j.progpolymsci.2013.06.006

de Oliveira, C. R. S., Batistella, M. A., de Souza, A. A. U., & de Souza, S. M.d. A. G. U. (2020). Synthesis of superacid sulfated TiO2 prepared by sol-gel method and its use as a titania precursor in obtaining a kaolinite/TiO2 nano-hybrid composite. *Powder Technology, 378*(Part A). https://doi.org/10.1016/j.powtec.2020.11.063

De Oliveira, C. R. S., Batistella, M. A., Lourenço, L. A., de Souza, S. M.d. A. G. U., & de Souza, A. A. U. (2021). Cotton fabric finishing based on phosphate/clay mineral by direct-coating technique and its influence on the thermal stability of the fibers. *Progress in Organic Coatings, 150*(August 2020), 105949. https://doi.org/10.1016/j.porgcoat.2020.105949

De Oliveira, C. R. S., Batistella, M. A., Souza, D., de A. G, U., S. M., & De Souza, A. A. U. (2017). Development of flexible sensors using knit fabrics with conductive polyaniline coating and graphite electrodes. *Journal of Applied Polymer Science, 134*(18), 1–10. https://doi.org/10.1002/app.44785

Dědková, K., Matějová, K., Lang, J., Peikertová, P., Kutláková, K. M., Neuwirthová, L., … Kukutschová, J. (2014). Antibacterial activity of kaolinite/nanoTiO2 composites in relation to irradiation time. *Journal of Photochemistry and Photobiology B: Biology, 135*, 17–22. https://doi.org/10.1016/j.jphotobiol.2014.04.004

Egyed, O., & Simon, J. (1979). Investigations on the flame-retardation of cellulosic fibrous materials - II. Investigation of the dehydration process. *Journal of Thermal Analysis, 16*(2), 321–327. https://doi.org/10.1007/BF01910694

FAO ICAC. (2013). *World apparel Fiber consumption survey*. Agriculture, Food and the, Organization of and, United Nations Cotton, International Committee, Advisory.

Gaan, S., & Sun, G. (2007a). Effect of phosphorus and nitrogen on flame retardant cellulose: A study of phosphorus compounds. *Journal of Analytical and Applied Pyrolysis, 78*(2), 371–377. https://doi.org/10.1016/j.jaap.2006.09.010

Gaan, S., & Sun, G. (2007b). Effect of phosphorus flame retardants on thermo-oxidative decomposition of cotton. *Polymer Degradation and Stability, 92*(6), 968–974. https://doi.org/10.1016/j.polymdegradstab. 2007.03.009

Gallo, E., Braun, U., Schartel, B., Russo, P., & Acierno, D. (2009). Halogen-free flame retarded poly(butylene terephthalate) (PBT) using metal oxides/PBT nanocomposites in combination with aluminium phosphinate. *Polymer Degradation and Stability, 94*(8), 1245–1253. https://doi.org/10.1016/j.polymdegradstab.2009.04.014

Gallo, E., Schartel, B., Acierno, D., & Russo, P. (2011). Flame retardant biocomposites: Synergism between phosphinate and nanometric metal oxides. *European Polymer Journal, 47*(7), 1390–1401. https://doi.org/10.1016/j.eurpolymj.2011.04.001

Grancaric, A. M., Tarbuk, A., & Pusic, T. (2005). Electrokinetic properties of textile fabrics. *Coloration Technology, 121*(4), 221–227. https://doi.org/10.1111/j.1478-4408.2005.tb00277.x

Günther, J., Thevs, N., Gusovius, H.-J., Sigmund, I., Brückner, T., Beckmann, V., & Abdusalik, N. (2017). Carbon and phosphorus footprint of the cotton production in Xinjiang, China, in comparison to an alternative fibre (Apocynum) from Central Asia. *Journal of Cleaner Production, 148*, 490–497. https://doi.org/10.1016/j.jclepro.2017.01.153

Hai, Y., Li, X., Wu, H., Zhao, S., Deligeer, W., & Asuha, S. (2015). Modification of acid-activated kaolinite with TiO2 and its use for the removal of azo dyes. *Applied Clay Science, 114*, 558–567. https://doi.org/10.1016/j.clay.2015.07.010

Hajj, R., El Hage, R., Sonnier, R., Otazaghine, B., Rouif, S., Nakhl, M., & Lopez-Cuesta, J.-M. (2020). Influence of lignocellulosic substrate and phosphorus flame retardant type on grafting yield and flame retardancy. *Reactive and Functional Polymers, 153*, 104612. https://doi.org/10.1016/j.reactfunctpolym.2020.104612

Kilinc, F. S. (Ed.). (2013). *Handbook of Fire Resistant Textiles* (1st ed.). The Textile Institute and Woodhead Publishing.

Harlin, A. (2019). Cellulose carbamate: Production and applications. In VTT Technical Research Centre of Finland (1st ed., issue 2019). VTT Technical Research Centre of Finland. Doi:10.32040/2019.978-951-38-8707-0.

Horrocks, A. R. (1983). An introduction to the burning behaviour of cellulosic fibres. *Journal of the Society of Dyers and Colourists, 99*(7–8), 191–197. https://doi.org/10.1111/j.1478-4408.1983.tb03686.x

Horrocks, A. R., Kandola, B. K., Davies, P. J., Zhang, S., & Padbury, S. A. (2005). Developments in flame retardant textiles – A review. *Polymer Degradation and Stability, 88*(1), 3–12. https://doi.org/10.1016/j.polymdegradstab. 2003.10.024

Huang, S., Wang, L., Liu, L., Hou, Y., & Li, L. (2015). Nanotechnology in agriculture, livestock, and aquaculture in China. A review. In *, Vol. 35, Issue 2. Agronomy for Sustainable Development*. https://doi.org/10.1007/s13593-014-0274-x

Huang, S., Feng, Y., Li, S., Zhou, Y., Zhang, F., & Zhang, G. (2019). A novel high whiteness flame retardant for cotton. *Polymer Degradation and Stability, 164*, 157–166. https://doi.org/10.1016/j.polymdegradstab. 2019.03.014

Jabli, M., Tka, N., Ramzi, K., & Saleh, T. A. (2018). Physicochemical characteristics and dyeing properties of lignin-cellulosic fibers derived from Nerium oleander. *Journal of Molecular Liquids, 249*, 1138–1144. https://doi.org/10.1016/j.molliq.2017.11.126

Jose, S., Shanmugam, N., Das, S., Kumar, A., & Pandit, P. (2019). Coating of lightweight wool fabric with nano clay for fire retardancy. *Journal of the Textile Institute, 110*(5), 764–770. https://doi.org/10.1080/00405000.2018.1516529

Kafle, K., Greeson, K., Lee, C., & Kim, S. H. (2014). Cellulose polymorphs and physical properties of cotton fabrics processed with commercial textile mills for mercerization and liquid ammonia treatments. *Textile Research Journal, 84*(16), 1692–1699. https://doi.org/10.1177/0040517514527379

Kibanova, D., Trejo, M., Destaillats, H., & Cervini-Silva, J. (2009). Synthesis of hectorite-TiO2 and kaolinite-TiO2 nanocomposites with photocatalytic activity for the degradation of model air pollutants. *Applied Clay Science, 42*(3–4), 563–568. https://doi.org/10.1016/j.clay.2008.03.009

Kiliaris, P., & Papaspyrides, C. D. (2010). Polymer/layered silicate (clay) nanocomposites: An overview of flame retardancy. *Progress in Polymer Science, 35*(7), 902–958. https://doi.org/10.1016/j.progpolymsci.2010.03.001

Klemm, D., Heublein, B., Fink, H.-P., & Bohn, A. (2005). Cellulose: Fascinating biopolymer and sustainable raw material. *Angewandte Chemie International Edition, 44*(22), 3358–3393. https://doi.org/10.1002/anie.200460587

Kottegoda, N., Sandaruwan, C., Perera, P., Madusanka, N., & Karunaratne, V. (2015). Modified layered nanohybrid structures for the slow release of urea. *Nanoscience &Nanotechnology-Asia, 4*(2), 94–102. https://doi.org/10.2174/2210681204021505211247 29

Laachachi, A., Cochez, M., Leroy, E., Ferriol, M., & Lopez-Cuesta, J. M. (2007). Fire retardant systems in poly(methyl methacrylate): Interactions between metal oxide nanoparticles and phosphinates. *Polymer Degradation and Stability, 92*(1), 61–69. https://doi.org/10.1016/j.polymdegradstab. 2006.09.011

Laachachi, A., Leroy, E., Cochez, M., Ferriol, M., & Lopez Cuesta, J. M. (2005). Use of oxide nanoparticles and organoclays to improve thermal stability and fire retardancy of poly(methyl methacrylate). *Polymer Degradation and Stability, 89*(2), 344–352. https://doi.org/10.1016/j.polymdegradstab. 2005.01.019

Laoutid, F., Bonnaud, L., Alexandre, M., Lopez-Cuesta, J. M., & Dubois, P. (2009). New prospects in flame retardant polymer materials: From fundamentals to nanocomposites. *Materials Science and Engineering R: Reports, 63*(3), 100–125. https://doi.org/10.1016/j.mser.2008.09.002

Lee, C. M., Mittal, A., Barnette, A. L., Kafle, K., Park, Y. B., Shin, H., … Kim, S. H. (2013). Cellulose polymorphism study with sum-frequency-generation (SFG) vibration spectroscopy: Identification of exocyclic CH2OH conformation and chain orientation. *Cellulose, 20*(3), 991–1000. https://doi.org/10.1007/s10570-013-9917-3

Lewin, M. (2001). Synergism and catalysis in flame retardancy of polymers. *Polymers for Advanced Technologies, 12*(3–4), 215–222. https://doi.org/10.1002/pat.132

Li, C., Sun, Z., Dong, X., Zheng, S., & Dionysiou, D. D. (2018). Acetic acid functionalized TiO2/kaolinite composite photocatalysts with enhanced photocatalytic performance through regulating interfacial charge transfer. *Journal of Catalysis, 367*, 126–138. https://doi.org/10.1016/j.jcat.2018.09.001

Liang, S., Neisius, M., Mispreuve, H., Naescher, R., & Gaan, S. (2012). Flame retardancy and thermal decomposition of flexible polyurethane foams: Structural influence of organophosphorus compounds. *Polymer Degradation and Stability, 97*(11), 2428–2440. https://doi.org/10.1016/j.polymdegradstab. 2012.07.019

Lopez-Cuesta, J.-M. (2017). Flame retardancy properties of clay–polymer nanocomposites. In *Clay-polymer nanocomposites* (pp. 443–473). Elsevier. https://doi.org/10.1016/B978-0-323-46153-5.00013-6.

Luxbacher, T. (2014). *The ZETA Guide: Principles of the streaming potential technique* (1 st). (Anton Paar GmbH).

Mamulová Kutlákova, K., Tokarský, J., Kovář, P., Vojtěšková, S., Kovářová, A., Smetana, B., Kukutschová, J., Čapková, P., & Matějka, V. (2011). Preparation and characterization of photoactive composite kaolinite/TiO2. *Journal of Hazardous Materials, 188*(1–3), 212–220. https://doi.org/10.1016/j.jhazmat.2011.01.106

Mansikkamäki, P., Lahtinen, M., & Rissanen, K. (2007). The conversion from cellulose I to cellulose II in NaOH mercerization performed in alcohol-water systems: An X-ray powder diffraction study. *Carbohydrate Polymers, 68*(1), 35–43. https://doi.org/10.1016/j.carbpol.2006.07.010

Menachem, L., & Pearce, E. M. (2006). *Handbook of fiber chemistry* (3nd ed.). Taylor & Francis.

Mistry, B. D. (2009). A handbook of spectroscopic data - chemistry. In *Oxford Book Company*.

Mngomezulu, M. E., John, M. J., Jacobs, V., & Luyt, A. S. (2014). Review on flammability of biofibres and biocomposites. *Carbohydrate Polymers, 111*, 149–182. https://doi.org/10.1016/j.carbpol.2014.03.071

Moltó, J., Conesa, J. A., Font, R., & Martín-Gullón, I. (2005). Organic compounds produced during the thermal decomposition of cotton fabrics. *Environmental Science & Technology, 39*(14), 5141–5147. https://doi.org/10.1021/es0482435

Montazer, M., & Harifi, T. (2018). Flame-retardant textile nanofinishes. In *Nanofinishing of Textile Materials* (1st ed., pp. 163–181). The Textile Institute Book Series and Elsevier. https://doi.org/10.1016/B978-0-08-101214-7.00011-X.

Morgan, A. B., & Wilkie, C. A. (2007). *Flame retardant polymer nanocomposites*. John Wiley & Sons.

Nam, S., Condon, B. D., White, R. H., Zhao, Q., Yao, F., & Cintrón, M. S. (2012). Effect of urea additive on the thermal decomposition kinetics of flame retardant greige cotton nonwoven fabric. *Polymer Degradation and Stability, 97*(5), 738–746. https://doi.org/10.1016/j.polymdegradstab. 2012.02.008

Olawoyin, R. (2018). Nanotechnology: The future of fire safety. *Safety Science, 110* (August), 214–221. https://doi.org/10.1016/j.ssci.2018.08.016

Parikh, D. V., Thibodeaux, D., Sachinvala, N., Moreau, J. P., Robert, K. Q., Sawhney, A. P. S., & Goynes, W. R. (2006). Effect of cotton fiber mercerization on the absorption properties of cotton nonwovens. *AATCC Review, 6*, 38–43.

Parvinzadeh Gashti, M., Elahi, A., & Parvinzadeh Gashti, M. (2013). UV radiation inducing succinic acid/silica–kaolinite network on cellulose fiber to improve the functionality. *Composites Part B: Engineering, 48*, 158–166. https://doi.org/10.1016/j.compositesb.2012.12.002

Passauer, L., & Bender, H. (2017). Functional group analysis of starches reacted with urea-phosphoric acid—Correlation of wet chemical measures with FT Raman spectroscopy. *Carbohydrate Polymers, 168*(March), 356–364. https://doi.org/10.1016/j.carbpol.2017.03.094

Peng, C., Xu, C., Liu, Q., Sun, L., Luo, Y., & Shi, J. (2017). Fate and transformation of CuO nanoparticles in the soil-rice system during the life cycle of Rice plants. *Environmental Science and Technology, 51*(9), 4907–4917. https://doi.org/10.1021/acs.est.6b05882

Ratajczak, I., Rzepecka, E., Woźniak, M., Szentner, K., & Mazela, B. (2015). The effect of alkyd resin on the stability of binding (3-aminopropyl) triethoxysilane with cellulose and wood. *Drewno*, *58*(195), 91–99. Doi:10.12841/wood.1644-3985.115.08.

Ribeiro, S. P.d. S., Cescon, L.d. S., Ribeiro, R. Q. C. R., Landesmann, A., Estevão, L. R. d. M., & Nascimento, R. S. V. (2018). Effect of clay minerals structure on the polymer flame retardancy intumescent process. *Applied Clay Science, 161*(January), 301–309. https://doi.org/10.1016/j.clay.2018.04.037

Ripoll, L., Bordes, C., Marote, P., Etheve, S., Elaissari, A., & Fessi, H. (2012). Electrokinetic properties of bare or nanoparticle-functionalized textile fabrics. *Colloids and Surfaces A: Physicochemical and Engineering Aspects, 397*, 24–32. https://doi.org/10.1016/j.colsurfa.2012.01.022

Saleh, T. A. (2011). The influence of treatment temperature on the acidity of MWCNT oxidized by HNO3 or a mixture of HNO3/H2SO4. *Applied Surface Science, 257*(17), 7746–7751. https://doi.org/10.1016/j.apsusc.2011.04.020

Saleh, T. A. (2018). Simultaneous adsorptive desulfurization of diesel fuel over bimetallic nanoparticles loaded on activated carbon. *Journal of Cleaner Production, 172*, 2123–2132. https://doi.org/10.1016/j.jclepro.2017.11.208

Saleh, T. A. (2020). Nanomaterials: Classification, properties, and environmental toxicities. *Environmental Technology & Innovation, 20*, 101067. https://doi.org/10.1016/j.eti.2020.101067

Saleh, T. A., & Gupta, V. K. (2012). Characterization of the chemical bonding between Al2O3 and nanotube in MWCNT/ Al2O3 nanocomposite. *Current Nanoscience, 8*(5), 739–743. https://doi.org/10.2174/157341312802884418

Sebeia, N., Jabli, M., Ghanmi, H., Ghith, A., & Saleh, T. A. (2021). Effective dyeing of cotton fibers using Cynomorium Coccineum L. peel extracts: Study of the influential factors using surface response methodology. *Journal of Natural Fibers, 18*(1), 21–33. https://doi.org/10.1080/15440478.2019.1612302

Skinner, L. C. (2011). Distributions of polyhalogenated compounds in Hudson River (New York, USA) fish in relation to human uses along the river. *Environmental Pollution, 159*(10), 2565–2574. https://doi.org/10.1016/j.envpol.2011.06.013

Suflet, D. M., Chitanu, G. C., & Popa, V. I. (2006). Phosphorylation of polysaccharides: New results on synthesis and characterisation of phosphorylated cellulose. *Reactive and Functional Polymers, 66*(11), 1240–1249. https://doi.org/10.1016/j.reactfunctpolym.2006.03.006

Takigami, H., Suzuki, G., Hirai, Y., & Sakai, S. (2009). Brominated flame retardants and other polyhalogenated compounds in indoor air and dust from two houses in Japan. *Chemosphere, 76*(2), 270–277. https://doi.org/10.1016/j.chemosphere.2009.03.006

Thompson, O. F., Galea, E. R., & Hulse, L. M. (2018). A review of the literature on human behaviour in dwelling fires. *Safety Science, 109*(March), 303–312. https://doi.org/10.1016/j.ssci.2018.06.016

Tka, N., Jabli, M., Saleh, T. A., & Salman, G. A. (2018). Amines modified fibers obtained from natural Populus tremula and their rapid biosorption of acid blue 25. *Journal of Molecular Liquids, 250*, 423–432. https://doi.org/10.1016/j.molliq.2017.12.026

Tokarský, J., Čapková, P., & Burda, J. V. (2012). Structure and stability of kaolinite/TiO2 nanocomposite: DFT and MM computations. *Journal of Molecular Modeling, 18*(6), 2689–2698. https://doi.org/10.1007/s00894-011-1278-y

Uddin, F., Areeb, T., Hussain, A., & Nadeem, A. (2015). Local clay mineral in flame retardant finishing of cotton fabric. *Chemical and Materials Engineering, 3*(1), 6–15. https://doi.org/10.13189/cme.2015.030102

Verbič, A., Gorjanc, M., & Simončič, B. (2019). Zinc oxide for functional textile coatings: Recent advances. *Coatings, 9*(9), 550. https://doi.org/10.3390/coatings9090550

Wang, C., Shi, H., Zhang, P., & Li, Y. (2011). Synthesis and characterization of kaolinite/TiO2 nano-photocatalysts. *Applied Clay Science, 53*(4), 646–649. https://doi.org/10.1016/j.clay.2011.05.017

Wang, Y., Wang, A., Wang, C., Cui, B., Sun, C., Zhao, X., Zeng, Z., Shen, Y., Gao, F., Liu, G., & Cui, H. (2017). Synthesis and characterization of emamectin-benzoate

slow-release microspheres with different surfactants. *Scientific Reports, 7*(1), 1–9. https://doi.org/10.1038/s41598-017-12724-6

Yun, Y. J., Lee, H. J., Son, T. H., Son, H., & Jun, Y. (2019). Mercerization to enhance flexibility and electromechanical stability of reduced graphene oxide cotton yarns. *Composites Science and Technology, 184*(September), 107845. https://doi.org/10.1016/j.compscitech.2019.107845

Zhao, B., Liu, Y.-T., Zhang, C.-Y., Liu, D.-Y., Li, F., & Liu, Y.-Q. (2017). A novel phosphoramidate and its application on cotton fabrics: Synthesis, flammability and thermal degradation. *Journal of Analytical and Applied Pyrolysis, 125*(March), 109–116. https://doi.org/10.1016/j.jaap.2017.04.011

Zhao, X. (2010). Synthesis and application of a durable phosphorus/silicon flame-retardant for cotton. *Journal of the Textile Institute, 101*(6), 538–546. https://doi.org/10.1080/00405000802563677

Zhu, P., Sui, S., Wang, B., Sun, K., & Sun, G. (2004). A study of pyrolysis and pyrolysis products of flame-retardant cotton fabrics by DSC, TGA, and PY–GC–MS. *Journal of Analytical and Applied Pyrolysis, 71*(2), 645–655. https://doi.org/10.1016/j.jaap.2003.09.005